The importance of allochthonous organic matter quality when investigating pulse disturbance events in freshwater lakes: a mesocosm experiment

Maria Calderó-Pascual · **Dilvin Yıldız** · **Gülce Yalçın** · **Melisa Metin** ·
Sinem Yetim · **Claudia Fiorentin** · **Mikkel René Andersen** · **Eleanor Jennings** ·
Erik Jeppesen · **Kemal Ali Ger** · **Meryem Beklioğlu** · **Valerie McCarthy**

Abstract Extreme precipitation is occurring with greater frequency and intensity as a result of climate change. Such events boost the transport of allochthonous organic matter (allo-OM) to freshwater ecosystems, yet little is known about the impacts on dissolved organic matter (DOM) quality and seston elemental stoichiometry, especially for lakes in warm climates. A mesocosm experiment located in a Turkish freshwater lake was designed to simulate a pulse event leading to increased inputs of allo-OM by examining the individual effects of increasing water colour (HuminFeed®, HF), the direct effects of the extra energetic inputs (alder tree leaf leachate, L), and the interactions of the single treatment effects (combination of both sources, HFL), along with a comparison with unmanipulated controls. Changes in the DOM quality and nutrient stoichiometry of the allo-OM treatment additions was examined over the course of the experiments. Results indicated that there was an

M. Calderó-Pascual (✉) · M. R. Andersen ·
E. Jennings · V. McCarthy
Centre for Freshwater and Environmental Studies,
Dundalk Institute of Technology,
Dundalk, Marshes Upper A91 K584, Co. Louth, Ireland
e-mail: maria.calderopascual@dkit.ie

D. Yıldız · G. Yalçın · M. Metin ·
S. Yetim · E. Jeppesen · M. Beklioğlu
Limnology Laboratory, Biological Sciences Department,
Middle East Technical University, 06800 Ankara, Turkey

G. Yalçın · E. Jeppesen · M. Beklioğlu
Ecosystem Research and Implementation Centre
(EKOSAM), Middle East Technical University,
06800 Ankara, Turkey

C. Fiorentin
Public Institution Natura Histrica, Riva 8, 52 100 Pula,
Croatia

E. Jeppesen
Department of Bioscience and Arctic Research Centre
(ARC), Aarhus University, 8600 Silkeborg, Denmark

E. Jeppesen
Sino-Danish Centre for Education and Research (SDC),
Beijing, People's Republic of China

E. Jeppesen
Institute of Marine Sciences, Middle East Technical
University, 33731 Mersin, Turkey

K. A. Ger
Department of Ecology, Federal University of Rio Grande
Do Norte, Campus Universitário, Natal,
RN 59078-900, Brazil

increase of high recalcitrant DOM components in the HF treatment, in contrast to an increase in less aromatic microbially derived molecules for the L treatment. Unexpectedly, seston C:P ratios remained below a severe P-limiting threshold for plankton growth and showed the same temporal pattern in all mesocosms. In contrast, seston N:P ratios differed significantly between treatments, with the L treatment reducing P-limiting conditions, whilst the HF treatment increased them. The effects of the combined HFL treatment indicated an additive type of interaction and chlorophyll-*a* was highest in the HFL treatment. Our results demonstrate that accounting for the optical and stoichiometric properties of experimental allo-OM treatments is crucial to improve the capacity to explain extrapolated conclusions regarding the effects of climate driven flooding on freshwater ecosystems in response to global climate change.

Graphical abstract
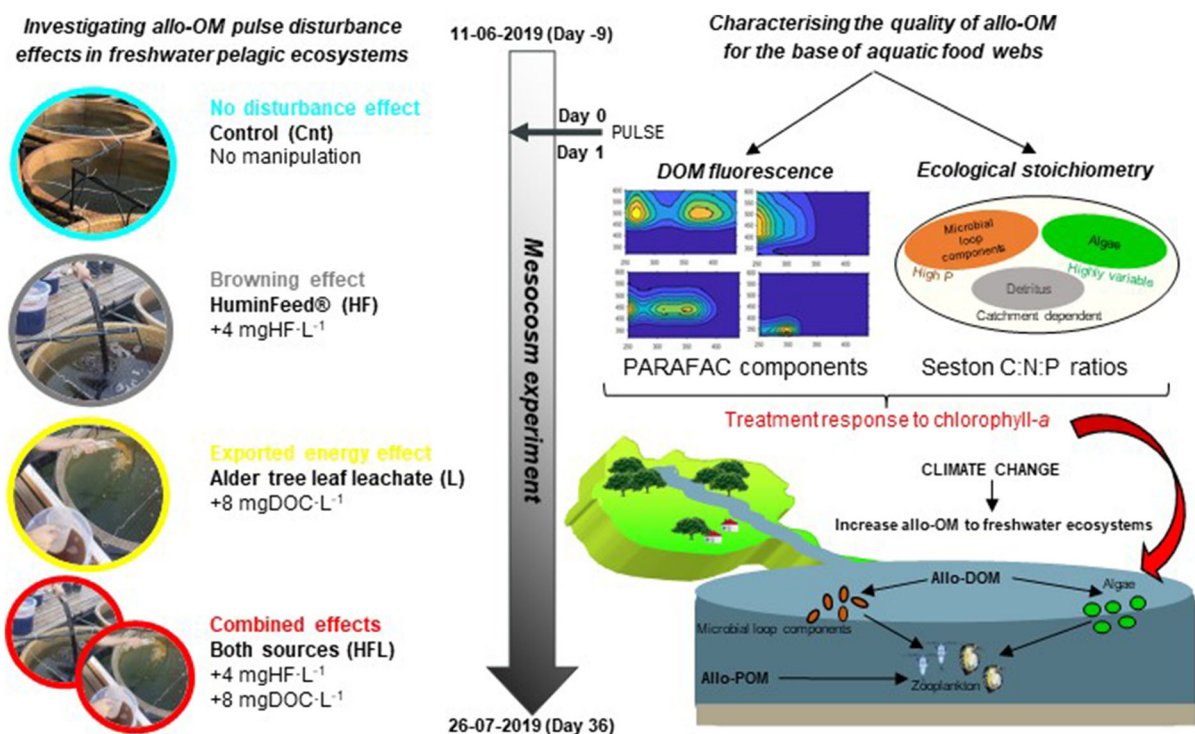
Introduction

Global climate change is altering precipitation patterns worldwide with reported widespread increases in both the frequency and intensity of daily rainfall (Toreti et al., 2013). Extreme precipitation events have become more intense in shorter time periods (Alpert et al., 2002). Consequently, there is a higher risk of flooding events but also more chances of summer droughts, which can directly affect soil moisture and stream flow (Cramer et al., 2018). Such conditions (i.e. warmer temperatures and intensified precipitation patterns) may boost the transport of terrestrial organic matter to freshwater ecosystems, varying in both quantity and quality, which are capable of producing cascade effects to aquatic food webs (Quante and Colijn, 2016).

Autochthonous organic matter (auto-OM) consists of carbon-based components directly derived from in-lake primary producers, mainly comprising biopoly-

mers of non-humic substances (Findlay & Sinsabaugh, 2003). Alternatively, allochthonous organic matter (allo-OM) is the fraction derived from the surrounding

terrestrial ecosystems, typically originating from plant tissues, and predominantly based on structural cellulose and lignin-like compounds (Thurman, 1985). Allo-OM loading in freshwater ecosystems has direct and indirect effects due to an increase in both water colour (a phenomenon referred to as 'browning') and the extra energetic input to the base of trophic food webs supporting catabolic (i.e. respired) and anabolic (i.e. biosynthesis) metabolisms (Solomon et al., 2015). Browning of freshwater bodies reduces euphotic depth, which can strongly limit phytoplankton growth and affect community composition depending on nutrient availability (Weyhenmeyer et al., 2016). In contrast, dissolved allo-OM can enhance heterotrophic bacteria productivity, selectively allocating this terrestrial dissolved organic carbon subsidy to biosynthesis (Guillemette et al., 2016). Furthermore, particulate (seston) allo-OM can be directly or indirectly (through microbial loop components) available to higher trophic levels, increasing or maintaining primary consumers biomass (Cole et al., 2011; Tanentzap et al., 2017).

Studies investigating the consequences of increased allo-OM loading in lakes tend to only focus on the quantity of dissolved organic carbon (DOC) fraction (Solomon et al., 2015; de Wit et al., 2016). Dissolved organic matter (DOM) quality, however, also plays a key role (Kothawala et al., 2014; Stadler et al., 2020). Intense rainfall events can drive shifts towards lower quality DOM molecular composition in freshwater bodies by relatively increasing concentrations of terrestrially derived high recalcitrant molecules (Zhou et al., 2020, 2021b), directly impacting microbe-mediated transformation of DOM and consequently altering energy flow through the base of aquatic ecosystems (Zhou et al., 2021a). The optical properties of DOM are related to its biochemical characteristics and, therefore, supply information on its origin and quality for planktonic communities (McKnight et al., 2001). These properties distinguish between coloured dissolved organic matter (CDOM), organic compounds that absorb light (chromophores), and fluorescent dissolved organic matter (FDOM), chromophores that re-emit light (fluorophores). Despite the complexity of DOM, specific patterns of FDOM have been associated with ecologically meaningful characteristics (Jaffé et al., 2014). Thus, FDOM constituents can range from humic-like fluorescence peaks strongly associated with high aromaticity, colour and highly persistent (i.e. difficult to degrade) poor-quality molecules mainly derived from terrestrial sources; to protein-like fluorescence peaks more associated with non-coloured, non-aromatic, and very labile (i.e. easy to degrade) high quality molecules mainly originating from in-lake primary producers (Fellman et al., 2010). For these reasons, efforts at understanding the effects of allo-OM loads to aquatic ecosystems would benefit from considering DOM quality in addition to its quantity.

Increases in extreme precipitation events leading to higher river inflows also mobilise particulate carbon (C) and export macro-nutrients such as nitrogen (N) and phosphorus (P) to lakes (Sebestyen et al., 2008; Dhillon & Inamdar, 2013). Factors controlling the type of allo-OM entering freshwater ecosystems are broad and catchment dependent (Qualls & Richardson, 2003). Phosphorus and N mobilisation mechanisms are complex, with a range of molecular weight distributions and consisting of both inorganic and organic fractions (Asam, 2012; Ged & Boyer, 2013; Kelly et al., 2019). Following high-intensity storms, particulate organic carbon (POC) export can be 6 to 8 times higher than DOC, dramatically altering the proportion of DOC and POC inputs to aquatic ecosystems (Dhillon & Inamdar, 2013; Hitchcock & Mitrovic, 2015). In addition, organic C exported from agricultural catchments after stormflows can produce a significant load (i.e. 50%) of relatively photoreactive and aromatic DOC into freshwater bodies (Caverly et al., 2013). In general, observations clearly indicate that POC and DOC can be highly mobilised during extreme rainfall events, with differences between relative contributions of dissolved and particulate fractions depending on the catchment type and land use (Hope et al., 1994; Jeong et al., 2012). In turn, N and P exports are also often higher during peak streamflow (Hitchcock & Mitrovic, 2015; Kelly et al., 2019). Indeed, dissolved nutrient subsides can have stimulatory (higher nutrient availability) and inhibitory (higher nutrient limitation) effects for primary producers and bacteria (Hitchcock & Mitrovic, 2015). In addition, examining elemental stoichiometry of seston is crucial for interpreting the effects of resource quality on zooplankton primary consumers (Sterner & Elser, 2002).

To date, laboratory experiments have been designed to better understand the complex effects of

allo-OM inputs on planktonic communities (Brett et al., 2009; Mcmeans et al., 2015; Vad et al., 2020). Furthermore, a commercially available humic substance called HuminFeed® (Humintech, Germany) has been widely used in mesocosm experiments investigating allo-OM inputs to lakes (Rasconi et al., 2015; Urrutia-Cordero et al., 2017; Lebret et al., 2018; Minguez et al., 2020). Considering the complexity of catchment-dependent allo-OM characteristics, other mesocosm studies have mimicked allo-OM using a range of different types of natural mixtures such as i) humic soil and inorganic N and P additions (Lefébure et al., 2013), ii) leaf leachate and inorganic N and P additions (Hitchcock et al., 2016; Brighenti et al., 2018; Tonetta et al., 2018), iii) filtered and concentrated humic lake water (Nicolle et al., 2012; Cooke et al., 2015; Hamdan et al., 2021), and iv) organic matter-rich top soils from inflowing rivers produced by preserving natural fine soil particles (Liess et al., 2015). In addition, in order to separate the browning effect from allo-OM as energy source effects, some authors simulated light reduction by adding a black net to reduce solar irradiance (Urabe et al., 2002; Brighenti et al., 2018).

Overall, experimental studies have shown that despite a general pattern of increasing heterotrophic activity following allo-OM disturbances in aquatic ecosystems, there are still a wide range of possible responses from primary producers and consumers. However, characterisation of DOM quality (Lennon et al., 2013) and changes in seston nutrient stoichiometry (Liess et al., 2015; Minguez et al., 2020) have received little attention, despite their potential importance in explaining the divergent findings regarding the effects of allo-OM on aquatic ecosystems (Creed et al., 2018; Senar et al., 2021). None of the published mesocosm experiments, to date, have attempted to characterise how quality features of different allo-OM sources would impact freshwater planktonic communities (Lennon & Cottingham, 2008; Geddes, 2015; Hitchcock et al., 2016; Lebret et al., 2018; Fonseca et al., 2022), despite the known variability of allo-OM sources in nature (Kellerman et al., 2014). Finally, studies of allo-OM pulses following extreme precipitation are scarce for lakes in warmer climates compared to those carried out in north temperate and boreal aquatic systems (Monteith et al., 2007; de Wit et al., 2016).

Experiments which address past experimental limitations are essential for gaining greater consensus on allo-OM effects to the base of aquatic pelagic food webs. Therefore, a mesocosm experiment located in a Turkish freshwater lake was carried out to explore the system responses to allo-OM pulse disturbance events. The experimental treatments were designed to examine the individual effects of increasing water colour (HuminFeed®, "HF"), the extra energetic inputs (alder tree leaf leachate, "L"), and the interactions of the single treatment effects (combination of both sources, "HFL"), along with a comparison with unmanipulated controls. Specifically, the work presented here aimed to first characterise the quality of different allo-OM source additions during the experiment by examining DOM fluorescence indicators and seston food quality for primary consumers (i.e. seston C:P and N:P ratios); to compare the overall treatment effects on water quality parameters with the log response ratio (LRR) detailed in Hillebrand & Gurevitch (2016); and subsequently, investigate the response in primary producers by examining chlorophyll-*a* (Chl-*a*) trends over the course of the experiment. We expected the following:

i. The HF treatment would increase water colour and provide a low quantity of high recalcitrant DOM (Lebret et al., 2018), compared to the L treatment that would add higher quantities of more labile DOM, without significantly increasing water colour (Hitchcock et al., 2016), relative to controls.

ii. The HF treatment would directly increase seston C:P ratios, without affecting seston N:P composition (Minguez et al., 2020), whilst the L treatment would add both seston C and P (Navarro et al., 2019), increasing seston C:P ratios, but less than in the HF treatment, and reduce seston N:P, relative to controls.

iii. Synergistic interactions would prevail in the combined HFL treatment in that DOM fluorescence indicators and seston elemental ratios LRR effects would be significantly greater than the addition of the respective single treatments due to biotic and abiotic processes occurring when both sources were mixed.

iv. Chl-*a* would, relative to the controls, decrease in the HF treatment due to light and nutrient constraints (Lefébure et al., 2013; Rasconi et al.,

2015), and increase in the L treatment due to nutrient additions arising from the leaf leachate and low light limitation compared to the HF treatment (Hitchcock et al., 2016; Brighenti et al., 2018). In the combined HFL treatment we expected Chl-*a* to remain higher than the HF but lower than the L treatments due to single treatment counteracting effects (i.e. increase of light limitation but addition of nutrients).

Methods

Study area and experimental design

At the beginning of June 2019, 16 cylindrical fibre-glass enclosures (1.2 m diameter × 2.2 m height × 4 mm thick) were fixed on a floating platform called *Middle East Technical University (METU) Mesocosm System* (39° 52′ 13.18″ N, 32° 46′ 31.92″ E), in Ankara, Turkey. The experimental set-up consisted of a control and three different treatments in a 4 × 4 factorial design (i.e. 4 treatments and 4 replicates per treatment). Water from the experimental lake, sieved through a 500 μm mesh, was used to fill the enclosures (2480 L initial volume) and ensure a natural chemistry of the water (Landkildehus et al., 2014). A water pump (3 W, Sobo wp-50M) was placed in the middle of each enclosure (150 cm below surface water) to ensure sufficient mixing of the whole water volume (i.e. avoiding water column stratification and sedimentation processes). A bird protecting net (3 × 3 cm mesh size) was placed on top to prevent the entrance of any bigger entity. The mesocosms did not include sediments, macrophytes, or fish to target effects on pelagic planktonic ecosystems. Mesocosms were inoculated on the 11th of June with a mixed sample of phytoplankton and zooplankton communities from five other nearby lakes whose trophic states varied from oligotrophic to eutrophic. To collect inoculated phytoplankton samples, 10 l of whole water column from the five other nearby lakes using a Ruttner sampler were sieved through 55 μm mesh to remove zooplankton and prevent grazing of phytoplankton before inoculation of mesocosms. For inoculated zooplankton samples, five vertical hauls covering the entire water column and single horizontal haul over the longest horizontal transect of the lake were taken by using a 55 μm mesh plankton net. Concentrated zooplankton samples were stored in 10 l of surface lake water before inoculation of mesocosms. Until the inoculation day (maximum 3 days after collection), the plankton samples were oxygenated (via gentle bubbling) and kept in a temperature controlled (22 ± 1 °C) room under low, indirect light. For the inoculation, planktonic samples were pooled together and well mixed. Two litres of the planktonic sample were added into each mesocosms. After inoculation, the mesocosms were incubated for a period of nine days before the pulse disturbance event to allow potential development of a diverse planktonic community with similar starting conditions. The additions of the three different allo-OM sources were carried out on the 20th of June (day 0). After the pulse disturbance the experiment ran until day 36, the 26th of July.

Allo-OM treatments

HuminFeed® is a commercially available lignite derived product and its detailed chemical composition has been fully characterised by Meinelt et al. (2007). In our experiment, the HuminFeed® stock solution was freshly prepared a few hours before the pulse by manually mixing for approximately 30 min at room temperature 99.2 g of HuminFeed® powder (stored in the fridge at 4 °C) in 40 l of distilled water (at room temperature). Final HuminFeed® stock solution concentration was 2480 mgHF l^{-1}. To simulate local terrestrial carbon sources, approximately 12 kg of fresh alder leaves were collected and spread out evenly in a ventilated greenhouse to allow them to dry quickly for 48 h five days prior to the mesocosms additions. After the drying period, leaves were placed in a dark cold room (4 °C) with distilled water (30 g of dried leaves per each litre of distilled water added) for 48 h. Darkness and cold environment was chosen following methodology in previous studies (Hitchcock et al., 2016; Fonseca et al., 2022) to reduce biotic and abiotic degradation of the prepared leaf leachate. After sieving the leaves from the water through 45 μm mesh size to exclude larger leaf material, a final stock solution was produced with a final DOC concentration of 2506 mgC l^{-1}. Alder tree leaf leachate was chosen because it had been used in similar studies, could be found in a nearby forested area, and were logistically viable to obtain enough DOC concentration of the stock solution in a relative short period of time

(Mutschlecner et al., 2018). Therefore, both stock solutions were added to the respective mesocosms immediately after preparation without any further sterilisation (i.e. autoclave) either filtration (i.e. through 0.22–0.45 μm) processes, such as carried out in other studies (Nicolle et al., 2012; Geddes, 2015; Brighenti et al., 2018). The experimental setup consisted of four replicates for each of the following treatments applying concentrations used in other published work: (1) unmanipulated controls (Cntl); (2) the HF treatment which received 4 l of Humin-Feed® stock solution resulting in a final HuminFeed® addition of 4 mgHF l^{-1} (equivalent to ~ 1.5 mgC l^{-1} as DOC) to increase water colour (Urrutia-Cordero et al., 2017; Lebret et al., 2018); (3) the L treatment by adding 7.9 l of alder tree leaf extract stock solution resulting in a corresponding added DOC concentration of ~ 8 mgC l^{-1} to test for an extra energetic input (Hitchcock et al., 2016); and (4) the combined HFL treatment composed of the same volume of stock solutions as added in the individual treatments, resulting in a pulse addition of 4 l of HuminFeed® stock solution (addition of ~ 1.5 mgC l^{-1} as DOC) and 7.9 l of alder tree leaf extract stock solution (addition of ~ 8 mgC l^{-1} as DOC) to compare the interactions of the single treatment effects (Fonseca et al., 2022). Owing to the focus on examining qualitative characteristics of the allo-OM, DOC quantities in this study are not directly comparable.

Mesocosm sampling strategy

Dissolved, seston, total C, N, and P, and Chl-*a* were measured every 4 days. In addition, parameters were sampled before (i.e. day 0) and after (i.e. day 1) the pulse treatment additions. The enclosures were sampled from the surface to the bottom using integrated tube samplers (one tube per treatment to avoid contamination). For each enclosure, three depth-integrated samples were taken across the diameter of each mesocosm and were pooled in 15 l plastic buckets. A subsample of the mixed water was transferred to acid washed 500 ml plastic bottles for water chemistry analyses. Three litres of 45 μm pre-sieved water was transferred to pre-washed plastic bottles to collect the seston fraction. Collected samples were stored in dark in a cooler until further analyses or preservation step in the laboratory (within 3–4 h).

Laboratory analyses

Dissolved samples were obtained by filtering water through Whatman GF/C glass fibre filters. Dissolved organic carbon concentrations were analysed with a Shimadzu TOC-L/CPN analyser (Schimadzu Scientific Instruments, Japan). Total nitrogen (TN; unfiltered), ammonium ($NH4^+$; filtered), and nitrite–nitrate ($NO_{2,3}^-$ filtered) were determined using an automated wet chemistry analyser (San++, Skalar Analytical, The Netherlands) (Baird & Bridgewater, 2017). Ammonium, nitrite, and nitrate concentrations were summed and reported as dissolved inorganic nitrogen (DIN). Total phosphorus (TP; unfiltered) and soluble reactive phosphorous (SRP; filtered) concentrations were determined spectrophotometrically using the molybdenum blue method (Mackerth, 1978). Between 200 and 600 ml of pre-sieved water through a 45 μm mesh were filtered onto pre-combusted and pre-weighted Whatman GF/F glass fibre filters for seston C, N, and P content analyses. In total 2 filters per enclosure were collected (one for C and N analyses and the other for P analyses). Filters were immediately dried at 60 °C for 24 h and then weighted for dry weight calculations. Filters were preserved in dark at room temperature inside zip lock plastic bags until further analyses. Prior to C and N analyses, seston filters were left for 6 h in a desiccator containing a beaker of hydrochloric acid (HCL, 37%) to remove inorganic C (Harris et al., 2001). Filters were then measured for C and N content using an elemental analyser (vario EL cube, Elementar, Germany). Standard reagent used for this analysis was Acetanilide (C_8H_9NO) with a composition of 10.36% of N and 71.09% of C. Seston P content was determined as specified for TP following combustion at 550 °C for 2 h and digestion step with potassium persulfate under high pressure and temperature (Autoclave for 30 min at 15 psi and 121 °C). Three blank filters per batch were considered for all C, N, and P analyses (McCarthy et al., 2006). Chlorophyll-*a* samples were filtered onto Whatman GF/C glass fibre filters and then extracted with ethanol before reading the absorbances in a UV–Vis spectrophotometer (Perkin Elmer Lambda35) (limit of detection [LoD] of 0.04 μgChl-*a* l^{-1}) (Jespersen & Christoffersen, 1987).

Optical properties of DOM

For logistical reasons, only water samples from day 4 to day 24 were filtered through Whatman 0.45 μm filters to carry out full UV–Vis spectrophotometer scans and fluorescence excitation–emission matrices (EEMs). DOM absorbance was measured using an UV–Vis spectrophotometer (UV-1800, Shimadzu, Germany) carrying out full scans across wavelengths from 200 to 900 nm using 1 cm glass cuvette and Milli-Q water as blank. Absorbance units measured at 420 nm were used to characterise water colour as a proxy of brownification (Weyhenmeyer et al., 2016). Fluorescence EEMs were characterised using a fluorescence spectrophotometer (Varian Cary Eclipse, Agilent technologies, USA) in 1 cm quartz cuvette. Fluorescence intensities were measured at excitation wavelengths ranging from 220 to 450 nm (5 nm increments) and emission wavelengths ranging from 240 to 600 nm (2 nm increments). Fluorescence EEMs were analysed using the drEEM toolbox (Murphy et al., 2013) in MATLAB version R2020b (The Math Works, Inc., 2020) and available code can be found in supplementary material. EEMs were corrected for instrument-specific biases using manufacturer supplied instrument correction factors. Spectra were also blank subtracted and corresponding absorbance measurements were used to correct for inner filter effects. Arbitrary fluorescence intensities were then normalised to a standard scale of Raman Units (RU). Any residuals of Raman and Rayleigh non-trilinear scatter were removed, without further interpolating the missing values, before multivariate parallel factor analysis (PARAFAC) (Murphy et al., 2013). Specific fluorescence components were identified by carrying out PARAFAC models. These models assume that each EEM sample set can be decomposed depending on a predefined number of components (Murphy et al., 2013). Steps to design the optimal PARAFAC model include the following: (1) the identification and removal of outliers, (2) development of preliminary models to explore the appropriate number of components, (3) determination of the correct number of components by finding chemically meaningful spectral loadings, and (4) internal model validation using split-half analysis by comparing models with different subsets of the original data (Murphy et al., 2013). Accordingly, the best model identified four fluorescence components, labelled C1–C4. Components identified ranged from high recalcitrant humic-like substances of terrestrial origin to labile protein-like freshly produced components, C3, C1, C4, and C2, respectively (Table 1). Finally, the optimum validated PARAFAC model was exported to OpenFluor, an online repository of published organic fluorescence spectra, to link the mesocosm fluorescence DOM patterns with trends observed in other aquatic systems (Murphy et al., 2013). PARAFAC model will be publicly available in OpenFluor once it can be linked with a published study.

Statistical methods

Pairwise comparisons of the four different treatments (four-factor ANOVA), with the Bonferroni method to adjust P-values by the number of comparisons (Heckler, 2005), were applied to different nutrient fraction variables every sampling day of the experiment (days 0, 1, 4, 8, 12, 16, 20, 24, 28, 32, and 36) to determine statistical differences amongst treatments. Pairwise t-tests were performed using the t_test function in the rstatix package in R (Kassambara, 2020).

A non-metric multidimensional analysis (NMDS) followed by a pairwise adonis test was used to describe and compare changes in the PARAFAC components through the mesocosm experiment (from day 4 to day 24). A NMDS is a robust ordination technique based on a distance matrix by representing the pairwise (dis)similarity between samples in a low-dimensional space (Clarke, 1993). The Bray Curtis dissimilarity matrix was applied to relative intensity means of replicates of PARAFAC components which were fourth root transformed to down weigh the effect of the most dominant component. Samples that are ordinated closer to one another are likely to be more similar than those further apart. However, the scale of the axes of a NMDS is arbitrary as is the orientation of the plot. In addition, solutions with high stress values (usually > 0.2) should be interpreted with caution, whilst stress values < 0.05 indicate that the ordination is an excellent representation of the high-dimensional assemblage structure and there is low probability of misinterpretation (Buttigieg & Ramette, 2014). A pairwise adonis post-analysis was run to test for statistical differences between treatments (Anderson, 2017). The NMDS was computed with the function $metaMDS$ and the pairwise adonis test with the

function *pairwise.adonis* (Martinez Arbizu, 2017) of the vegan package in R (Oksanen, 2011).

We fitted generalised additive models (GAMs) with a Gaussian distribution (Wood, 2017) to seston nutrient ratios and Chl-*a* concentrations (all response variables were ln-transformed as recommended when dealing with nutrient ratios (Isles, 2020) and to avoid removal of Chl-*a* outliers). We analysed the effect of the treatments (factor variable of 4 levels) as well as temporal trends (i.e. days of the experiment: DOE) considering ordered-factor-smooth interaction and using the control treatment as the reference factor (Rose et al., 2012). After checking for the violation of the assumptions, if violated, we added a simple temporal correlation structure with the days of the experiment $(correlation = corAR1(form = \sim 1|DOE))$ to account for remaining temporal dependence of the observations (i.e. generalised additive mixed models, GAMMs). All GAM/Ms were carried out considering restricted maximum likelihood method (REML) as the parameter estimation procedure and optimum cubic regression splines (bs = 'cr') for the explanatory variables (Zuur et al., 2009). Specific mesocosm replicates' variability was checked by adding individual enclosures ($n = 16$) as a model smoother with random effect splines (bs = 're') (Pedersen et al., 2019), but these fixed random effects were dropped from all models as enclosures variability effects were insignificant. Models were compared by means of the Akaike Information Criterion (AIC), with lower AIC values indicating better models (Wood, 2017) (Table S2, S3, and S4). GAMs and GAMMs were performed using the *gam* and *gamm* functions, respectively, in the mgcv package in R (Wood & Wood, 2015).

A principal component analysis (PCA) was run to explore differences in mesocosm treatments based on colour, PARAFAC components, dissolved and seston nutrient concentrations and ratios as descriptors (15 variables), including sampling points from day 4 to day 24 and all treatment replicates ($n = 96$). The PCA summarises the general pattern between treatment observations and the available descriptive variables in a low-dimensional space illustrated as principal components and representing a high percentage variability of the data (Buttigieg & Ramette, 2014). The PCA was computed with the function *prcomp* in base R (R Core Team., 2019).

The magnitude of the effect of the addition of different allo-OM sources on carbon and nutrient quantity and quality parameters was calculated at each sampling time using the log response ratio (Wyatt & Rober, 2020). The LRR quantifies the proportionate change resulting from experimental manipulation and is calculated as the natural log (ln) of the treatment mean divided by the control mean (Hillebrand & Gurevitch, 2016). The direction of the effect size indicates whether the treatment had a positive or negative effect on the correspondent tested variable. In this study, calculated effect sizes at different days of the experiment have been grouped by treatments in boxplots of between 8 and 10 observations (n), depending on the variable studied and based on the sampling days, from day 1 to day 36. In turn, the respective LRR measures at day 0 (before allo-OM additions) were used as benchmarks and when day 0 was not available, the benchmark value was 0 (Hillebrand et al., 2018). With these effect sizes we wanted to test if, overall, (1) the treatment effects were significantly different from benchmark of day 0 and (2) the treatment effects were significantly different between treatments.

All R analyses were performed in version 4.0.3 (R Core Team., 2019) and available code can be found in supplementary material.

Results

Allo-OM additions

The initial (day 0, before treatment addition) DOC concentrations in all enclosures were the same, ranging from 3.4 to 2.2 mgC l^{-1}. Immediately following the allo-OM pulse (day 1), the mean ($\pm$ SD) DOC concentration significantly increased by 6.2 $\pm$ 1.4 mgC l^{-1} in the L (P-value < 0.05) and 6.6 $\pm$ 0.2 mgC l^{-1} in the HFL (P-value < 0.01) treatments, contrasting with insignificant changes in the HF treatment, relative to the control mesocosms (Fig. 1a; Table S1). The control treatment had a maximum DOC concentration of 5.4 $\pm$ 1.5 mgC l^{-1} at day 20 whilst HF enclosures had maximum values of 6.3 $\pm$ 1.4 mgC l^{-1} at day 28. In contrast, the DOC concentrations in the L and HFL treatments reached minimum values of 7.0 $\pm$ 0.1 mgC l^{-1} at day 36 and 6.3 $\pm$ 0.6 mgC l^{-1} at day 32, respectively (Fig. 1a).

The initial concentrations of seston C at day 0 were not significantly different across the treatments and varied between 0.6 and 0.9 mgC l^{-1}. The allo-OM additions then resulted in a significant increase of 0.3 ± 0.0 mgC l^{-1}, 0.4 ± 0.1 mgC l^{-1}, and 1.4 ± 0.2 mgC l^{-1}, respectively for the HF, L, and HFL treatments (P-values < 0.01; 0.01; 0.001) (Fig. 1b; Table S1). The seston C concentrations in the control mesocosms gradually decreased from 0.7 ± 0.1 to 0.3 ± 0.1 mgC l^{-1} during the experiment. In the HF, L, and HFL treatments, seston C also gradually decreased over the experiment to concentrations ranging from 0.3 to 0.5 mgC l^{-1} at day 36. None of the treatments were significantly different from the controls at the end of the experiment (Fig. 1b; Table S1).

HuminFeed® added significantly less water colour than the leaf leachate source (P-values < 0.01; 0.001 for HF and L, respectively), and colour in the HF treatment changed little throughout the experiment having an overall value of 0.007 ± 0.002 AU cm^{-1} (Fig. 1c; Table S1). In contrast, both the L and HFL treatments had the highest colour values immediately after the addition (Fig. 1c). Water colour of the L and HFL treatments decreased as the experiment progressed, from 0.018 ± 0.001 and 0.015 ± 0.001 AU cm^{-1} to 0.007 ± 0.003 and 0.013 ± 0.001 AU cm^{-1}, respectively, from day 4 to day 24. Water colour in the control treatment was significantly lower than all treatments throughout the experiment having an overall stable value of 0.001 ± 0.001 AU cm^{-1} (Fig. 1c; Table S1).

Initial DIN concentrations (day 0, before treatment addition) in all enclosures were highly variable and ranged from 15 to 117 µgN l^{-1}. Overall, the DIN pool did not increase after the allo-OM pulse disturbance (Fig. 1d). The HFL treatment had significant lower DIN concentrations at day 8 (P-value < 0.05), whilst the HF treatment had significant higher values at day 12 (P-value < 0.05), respective to controls (Fig. 1d; Table S1). For all treatments, the highest mean DIN values were observed between days 24 and 28. Final DIN concentrations in all mesocosms ranged from 37 to 83 µgN l^{-1}, which was within day 0 range (Fig. 1d). The initial seston N content of all replicates ranged from 325 to 649 µgN l^{-1}. The control treatment had a seston N minimum concentration of 219 ± 125 µgN l^{-1} at day 8 of the experiment, increasing again to the initial conc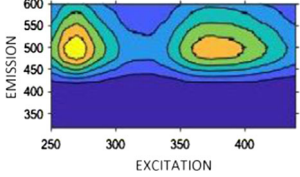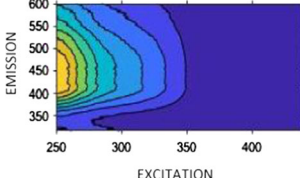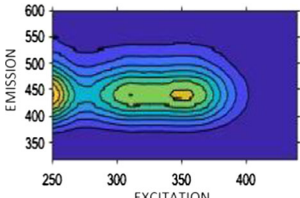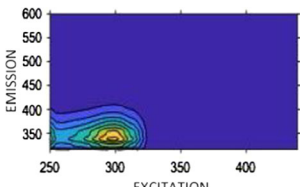entrations of 497 ± 65 µgN l^{-1} at the end of the experiment. After the allo-OM additions, the HF and L treatments experienced a similar increase in N concentration of 248 ± 208 and 356 ± 154 µgN l^{-1}, respectively. In the HFL treatment, seston N concentration increased to 676 ± 362 µgN l^{-1}. Only the L treatment increase was significant (P-value < 0.05) because the HF and HFL treatments experienced high variability amongst replicates (Fig. 1e; Table S1). At day 12, the seston N concentrations in the different treatments were already reduced to pre-disturbance conditions and remained stable until the end of the experiment (Fig. 1e). Total nitrogen values were highly variable amongst treatments. There was an overall increase in TN values in all mesocosms as the experiment progressed, with concentration ranging between 92 and 693 µgN l^{-1} from day 0 to day 36 (Fig. 1f; Table S1).

Unlike N, the HF treatment did not add more P to the system. Therefore, P fractions in the control and HF treatments remained constantly low and were not significantly different throughout the experiment (Fig. 1g, h, i; Table S1). The overall average SRP concentrations was 3.6 ± 3.2 µgP l^{-1} whilst the seston P content was 6.1 ± 4.4 µgP l^{-1}. In contrast, leaf leachate additions added P in both the L and HFL treatments, and increased the SRP and seston P concentrations of these two treatments by 18.4 ± 8.2 and 42.2 ± 11.7 µgP l^{-1}, respectively, from day 0 to day 1 (Fig. 1g, h; Table S1). Overall concentrations of SRP in the HFL treatment after the pulse remained high throughout the 36 days of the experiment (i.e. 19.4 ± 7.4 µgP l^{-1}), whilst SRP in the L treatment gradually decreased from 25.0 ± 5.5 µgP l^{-1} at day 1 to pre-pulse conditions (i.e. 2.8 ± 1.0 µgP l^{-1}) from day 20 onwards (Fig. 1g). The concentrations of seston P in the L and HFL treatments followed the same pattern, decreasing from maximum values at day 1 (i.e. 51.9 ± 10.5 µgP l^{-1}) to 7.0 ± 0.8 µgP l^{-1} at day 36 (Fig. 1h). In turn, TP values clearly replicated the pattern of the sum of the dissolved (SRP) and particulate (seston) fractions. Overall, the added P pool seemed to be consumed as the experiment progressed (Fig. 1i).

DOM quality

PARAFAC analysis of the fluorescent components of the DOM pool highlighted the dominance of more labile molecules (C2) in control mesocosms compared

Table 1 Fluorescence components modelled by PARAFAC and corresponding indication of molecule type and description according to literature [OpenFluor database and after Coble (1996)]

Component ID	Molecule type	Molecule description	Ex. Max. (nm)	EM. Max. (nm)	Parafac contours
C3	Humic-like	Terrestrial	270	500	
		High recalcitrant	370		
C1	Fulvic-like	Terrestrial	250	418	
		Less recalcitrant			
C4	Humic-like	Microbial	250	440	
		Less recalcitrant	355		
C2	Protein-like	Tryptophan	300	338	
		Labile			

Component EEM peaks and PARAFAC contours of emission and excitation matrices are given

with the allo-OM treatments (HF, L, and HFL) (Fig. 2). The HF treatment contained a high proportion of more recalcitrant humic-like molecules (C3 and C1). In contrast, the L treatment had a more even distribution of each of the four components, with a slightly greater prevalence of the less recalcitrant microbial derived humic-like C4 component (Fig. 2). In turn, the HFL treatment showed evidence indicating the presences of molecules from both the HF and L sources with an overall increase in humic-like components (C3, C1, and C4) (Fig. 2).

PARAFAC component composition revealed significant differences amongst treatments (pairwise adonis test, P-values < 0.05) (Fig. 3 and Fig. S1). The more labile protein-like C2 component found in all treatments (Fig. 2) dominated in the control enclosures during the whole study period (Fig. 3 and Fig. S1). The HFL treatment clustered with the C3 component whilst the HF treatment clustered closer to the C1 component, indicating a higher overall proportion of terrestrial humic-like and high recalcitrant poor-quality DOM in the HFL treatment (Fig. 3). In contrast, the L treatment grouped closer to the C4 component, which correspond to microbial humic-like, more labile DOM (Fig. 3 and Fig. S1). Temporal patterns from different treatments showed that, towards the end of the experiment, relative proportions of DOM components barely changed for each respective treatment obtaining different DOE observations grouped together to specific different components (Fig. 3 and Fig. S1).

Seston quality

Before the allo-OM pulse (day 0), all mesocosms experienced moderate P limitation based on published

seston C:P nutrient limitation thresholds for zooplankton primary consumers (ln-transformed seston C:P molar ratios > 4.86) (Hecky et al., 1993) (Fig. 4). Using GAMM models to assess temporal trends, all treatments were found to have the same significant temporal pattern in seston C:P (P-value < 0.01), with decreases occurring directly after the pulse additions, but gradually returning to pre-disturbance conditions during the experiment (Fig. 4; Table S2). In turn, the overall values in HF did not differ from controls, whilst being significantly lower in the L and HFL treatments (P-values < 0.001). At the end of the experiment, seston C:P in the controls and HF treatments approached the severe P-limitation threshold (ln-transformed seston C:P molar ratios > 5.56) for zooplankton herbivores (Urabe et al., 2002) (Fig. 4). The model explained 55.9% of the deviance in seston C:P ratios over the experimental days (Table S2).

Despite the allo-OM additions, seston N:P values of all enclosures remained above the theoretical severe seston P-limitation threshold, even though the treatments receiving the leaf leachate (i.e. L and HFL) had significant lower values of N:P relative to the control (P-values < 0.001), and the HF treatment significantly higher (P-value < 0.05) (Fig. 5; Table S3). In contrast to the seston C:P temporal dynamics, the trends in seston N:P for the L and HFL treatments were significantly different from the control (Fig. 5; Table S3). Seston N:P ratios gradually increased in the control and HF treatments during the experiment, specially between day 12 and 20. In the L treatment, seston N:P rapidly decreased after the pulse, but quickly increased to initial conditions by day 12 and remained high until the end of the experiment (P-value < 0.01). In contrast, the HFL treatment changes were weaker, with dynamics similar to the control and HF treatments but with absolute values resembling the L mesocosms (P-value < 0.05) (Fig. 5). Overall, this model explained 68.9% of the deviance in seston N:P ratios during the mesocosm experiment (Table S3).

Overall treatment effects

There was a clear separation between treatments with regards carbon and nutrient quality and quantity parameters (Fig. 6). The separation by the two principal components, PC1 with a weight of 49.7% and PC2 with a weight of 14.8%, was mediated mainly by

a differentiation in the DOM quality in both axis and by the additions of C and P fractions highly represented by PC1. Therefore, the control treatment observations clustered together and were characterised by relatively high concentrations of N compared to low P concentrations and a more labile DOM pool (C2). In turn, the HF treatment seemed to be differentiated by high seston C:P and N:P ratios and the recalcitrant fulvic-like DOM pool (C1) and, therefore, aggregated separately from the control samples. In contrast, the L treatment samples appeared aggregated in the opposite direction to the HF treatment and strongly associated with high colour, DOC and P concentrations. Finally, the HFL treatment observations grouped in between HF and L treatments and in the opposite direction to the control cluster, directly associated with high seston C, N, and P content and the high recalcitrant humic-like C3 DOM component (Fig. 6).

For all the included variables, which were those relating to carbon quantity as well as those related to nutrient seston quality and quantity, the HF treatment always had the lowest effect compared to the L and HFL treatments (Fig. 7a, b, d), with the exception of DOM quality high recalcitrant humic-like C3 and fulvic-like C1 components (Fig. 7c). In turn, the LRR effects of the HFL treatment indicated an additive type interaction (i.e. the sum of the effects of the treatments involved) with this treatment having more similar overall effects with the L than the HF treatments (i.e. LRR were not significantly different from the L treatment) (Fig. 7a, b, c, d). The LRR effect sizes of the seston elemental ratios showed that the HF and the treatments receiving the leaf leachate source evolved in opposite directions over the course of the experiment (i.e. positive vs negative LRR) (Fig. 7d).

Response of Chl-a

Chlorophyll-*a* temporal dynamics in the different treatments did not significantly differ from the control treatment. However, the L and HFL treatments had significantly higher Chl-*a* concentrations relative to the control (P-values < 0.05; 0.001, respectively). The GAM model explained 28.9% of the Chl-*a* deviance (Fig. 8; Table S7). Chlorophyll-*a* in all the enclosures during the experiment ranged from < LoD to 5.6 µgChl-*a* l^{-1} (Fig. 8). Before the pulse (day 0), overall Chl-*a* concentrations were low with
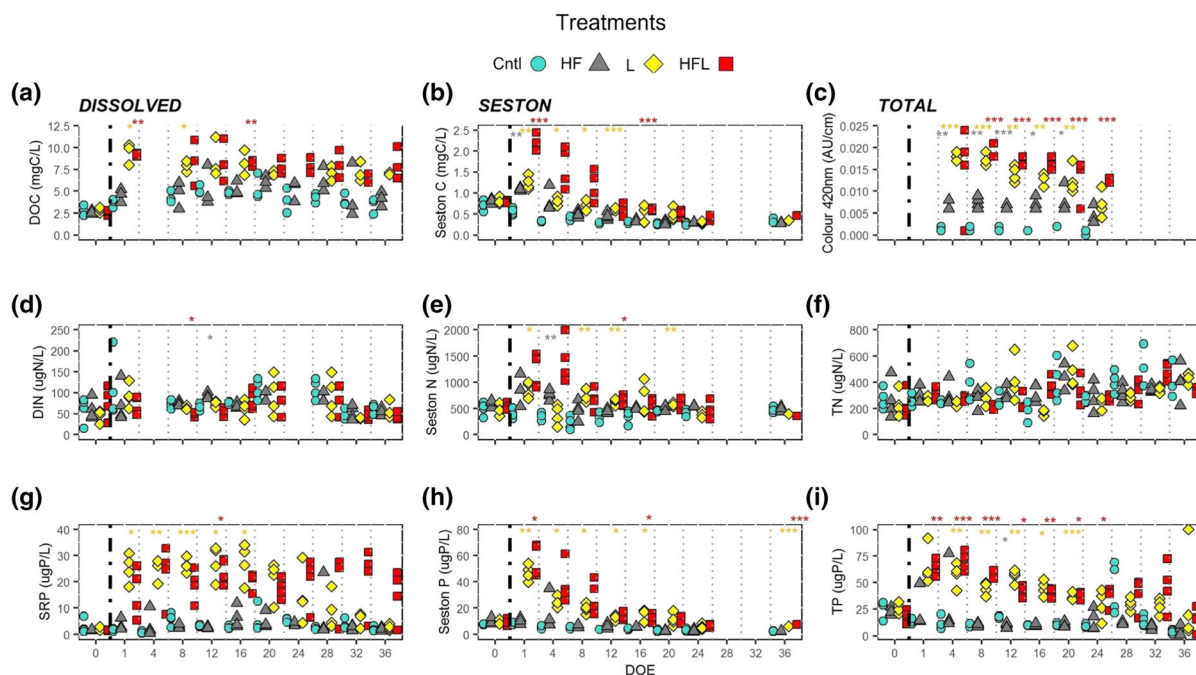
Fig. 1 Water quality dissolved, seston and total C, N, and P fractions during the mesocosm day of experiment (DOE; gaps when data not available): **a** DOC; **b** seston C; **c** colour; **d** DIN; **e** seston N; **f** TN; **g** SRP; **h** seston P; and **i** TP. Each point represents an observation (4 replicates per treatment per DOE). Treatments are represented in different shapes and colours: controls (Cntl) blue points, HuminFeed® (HF) grey triangles, leaf leachate (L) yellow diamonds, and combination of sources (HFL) red squares. Black dashed vertical line indicates when the

allo-OM pulse event occurred. Following grey dotted vertical lines separate each showed sampling day. Corresponding significant differences amongst treatments for each DOE can be found in Table S1. *P*-values significant codes differing from controls (Cntl): $P < 0.001$ = '***'; $P < 0.01$ = '**'; $P < 0.05$ = '*'; non-significant (Table S1). The treatment with significant difference is indicated by the respective colour (*grey* HF; *yellow* L; *red* HFL)

mean $\pm$ SD of 1.8 $\pm$ 1.0 µgChl-*a* l^{-1}. At day 12 all mesocosms reached minimum values < LoD. From day 16 to the end of the experiment Chl-*a* in the control and HF treatments remained low (i.e. 0.4 $\pm$ 0.5 µgChl-*a* l^{-1}). In contrast, from day 16 onwards, the treatments receiving the leaf leachate source (L and HFL) reached higher Chl-*a* concentrations of 1.0 $\pm$ 1.0 µgChl-*a* l^{-1}. The highest value of 5.6 µgChl-*a* l^{-1} in the HFL treatment was recorded at day 32, in only one replicate for this treatment (Fig. 8).

Discussion

As concerns relating to ongoing changes in allo-OM export to lakes and reservoirs have increased, there has been a parallel increase in the use of mesocosm studies to investigate these effects. Here we characterised the quality of different allo-OM additions to a mesocosm

experiment carried out in a warm climate freshwater lake. To our knowledge, this is the first study to examine changes in both the constituent DOM components and seston nutrient ratios of different allo-OM source additions over the course of a mesocosm experiment. We found that the different allo-OM sources resulted in significantly different treatment LRR effect sizes of the evaluated water quality aspects. These distinct treatment effect sizes should be key for understanding associated responses in the aquatic food web and elucidate divergent responses to these inputs within the system.

Importance of DOM quality along quantity

As expected, the addition of HuminFeed® increased the proportion of high recalcitrant DOM in the system, mainly the terrestrial fulvic-like C1 component and to a lesser degree the terrestrial humic-like C3

component. The humic-like C3 component has also been found in agricultural-forested catchments (Derrien et al., 2018), but in very low amounts compared to other components. On the other hand, the fulvic-like C1 component has been recurrently found in soil organic matter (Chai et al., 2019) and in a wide range of freshwater lakes and streams (Kida et al., 2019), being particularly dominant in forested and agricultural catchment streams (Stedmon and Markager, 2005). In our mesocosm experiment, C3 and C1 components that were associated with HF additions did not seem to be consumed by planktonic communities or to be abiotically degraded over the experiment. The leaf leachate source, on the other hand, enhanced the microbially derived humic-like C4 component, a fraction also found in yellow poplar leaf litter leachate (Wheeler et al., 2017), and has been observed in other studies using leaf leachate as a DOM

source (Cuss & Guéguen, 2015). High amounts of this component have been found across a diverse gradient of lakes in Greenland and it is particularly dominant in soil DOM extracts (Osburn et al., 2017). Other authors have related the C4 component to macrophyte DOM exudates, which are highly reactive to both sunlight and bacterial activity (Cory et al., 2013). To date, only one other mesocosm study has examined specific fluorescence properties (i.e. PARAFAC components) of different allo-OM treatments (Mutschlecner et al., 2018). Those authors identified PARAFAC components in leaf leachates derived from three different types of trees (i.e. alder, poplar, and spruce leaves). Similar to our study, they also found relatively high proportions of more labile DOM molecules, particularly for alder tree leaf leachates, the same type of leaves used in our experiment. Finally, in our study, the fact that all treatments maintained high proportions
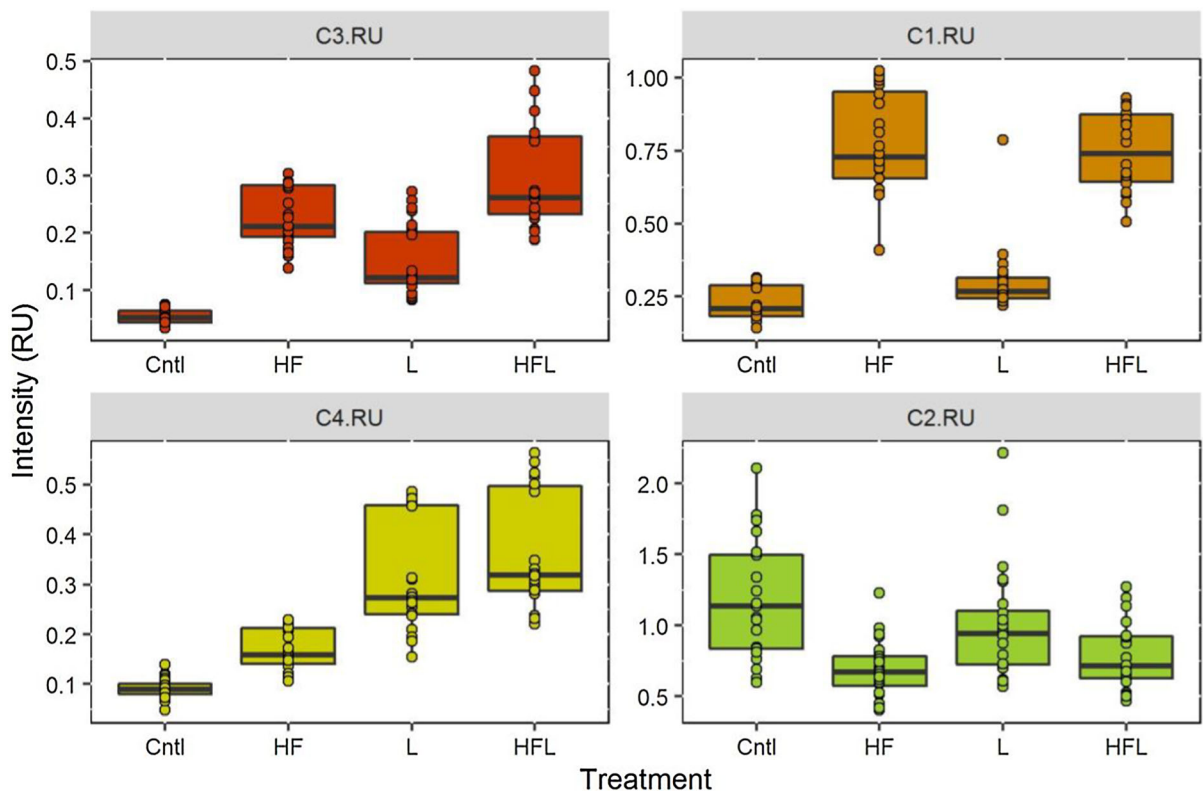

Fig. 2 Distribution of the intensity, in Raman Units (RU), of different PARAFAC components (C3, C1, C4, C2) in the four different treatments (*Cntl* controls, *HF* HuminFeed®, *L* leaf leachate, and *HFL* combination) from day 4 to day 24 of the experiment (n = 24 per treatment). The order of each PARAFAC component are based on the information provided in Table 1. From high recalcitrant humic-like component (C3), less recalcitrant terrestrial fulvic-like component (C1), microbial derived humic-like component (C4), to more labile protein-like component (C2). Box = 25th and 75th percentiles, whiskers = 1.5*inter-quartile range. Black line = median
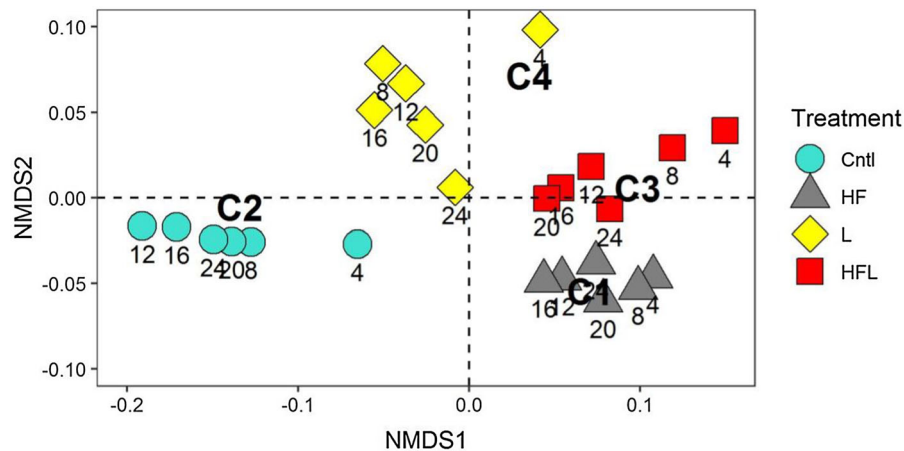
Fig. 3 Two-dimensional NMDS of the PARAFAC components based on 4th root transformed relative intensity of the mean of replicates per day of experiment (Fig. S1 represents the same without computing the mean of replicates). Treatment observations are represented in different colours and shapes: controls (Cntl) blue points, HuminFeed® (HF) grey triangles, leaf leachate (L) yellow diamonds, and combination (HFL) red squares. Specific day of experiment (4, 8, 12, 16, 20, and 24) is detailed in each observation point. The stress of the ordination is 0.026. Significant differences amongst treatments (pairwise adonis test with P-values < 0.05)

of the protein-like C2 component as the experiment progressed is supported by the observed increase in DOC concentrations in all treatments including the control treatment as the experiment progressed. The observed increase in DOC concentration in control enclosures that did not receive any allo-OM additions suggests that internal food web processes such as DOC exudation from algae or excretion from higher trophic levels were important contributors to DOC concentrations, as also reported in another similar experiment (Geddes, 2015). In our study, quantities of Humin-Feed® and leaf leachate were added based on previously published experiments utilising these allo-OM sources with similar designs (Geddes, 2015; Rasconi et al., 2015; Hitchcock et al., 2016; Urrutia-Cordero et al., 2017). The HF treatment added only small quantities of DOC, as was expected based on previous studies (Lebret et al., 2018; Minguez et al., 2020), compared with the higher quantities of DOC added from the leaf leachate source as intended based on the experimental design. Therefore, monitoring DOM quality in this study allowed individual DOM constituents in the different treatments to be elucidated, each of which will have differing outcomes and responses for planktonic communities. To this end, considering DOM quality and not just quantity allows for a better understanding of the consequences of increased allo-OM inputs to aquatic ecosystems.

Browning phenomenon

There are a number of approaches which can be used in order to examine the browning effect in aquatic systems which are thought to reduce light conditions for phytoplankton growth. These include the use of covers across the top of the treatment enclosures in order to reduce solar irradiation (Urabe et al., 2002; Villar-Argaiz et al., 2018). However, these methods may not properly mimic potential phytoplankton light limitation in aquatic ecosystems as predicted with increases in water colour. In addition, by using covers, algae growth could be unexpectedly enhanced due to a reduction of photo inhibitory effects, as found in a mesocosm study carried out in a tropical lake (Brighenti et al., 2018). HuminFeed® has previously been used to examine the browning effect in meso-cosm experiments (Urrutia-Cordero et al., 2017; Lebret et al., 2018) and was, therefore, chosen for this purpose in our experiment. The C1 fulvic-like component clearly increased in our HF treatment and it has been previously reported to have highly photorefractory components because of the rapid attenuation of UVB light in water which increases as bulk DOM photodegrades (Kida et al., 2019). This would reinforce our initial assumption that HF mimics well freshwater browning scenarios. However, in contrast to what we expected, and mainly due to
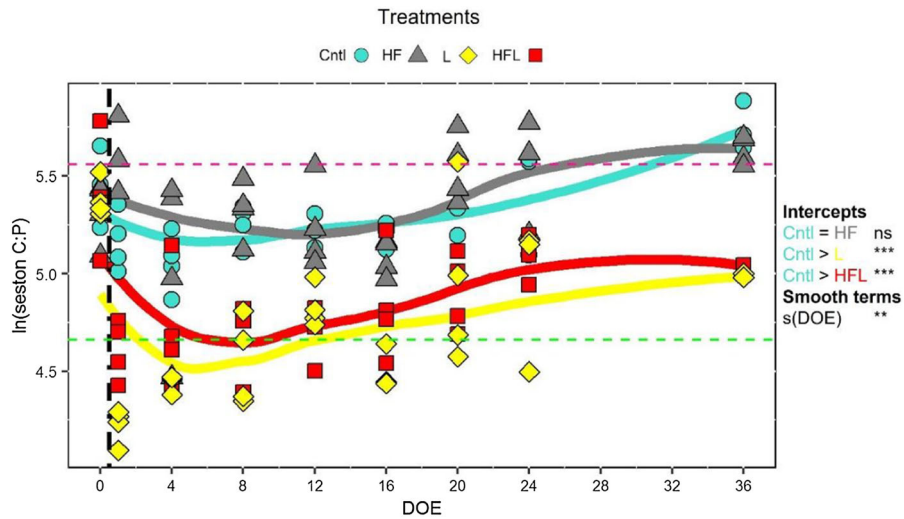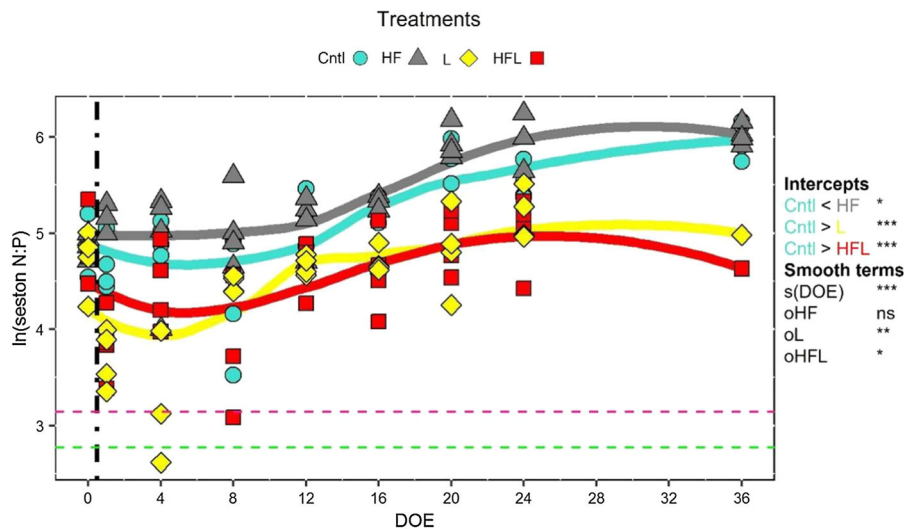
Fig. 4 GAMM smoothers (solid lines) showing the temporal trends in ln-transformed seston C:P ratios during the days of the experiment (DOE). Points are observations for each respective treatment (*Cntl* blue points, *HF* grey triangles; *L* yellow diamonds; *HFL* red squares). Green dashed horizontal line indicates the Redfield ratio (lnC:P = 4.66) and pink one the threshold elemental ratio for seston P nutrient deficiency, lnC:P > 5.56 (Healey & Hendzel, 1980). Black dashed vertical line indicates when the allo-OM pulse event occurred. Model summary output is in Table S2. *P*-values significant codes: < 0.001 = '***'; < 0.01 = '**'; < 0.05 = '*'; non-significant = ns

Fig. 5 GAM smoothers (solid lines) showing the temporal trends in ln-transformed seston N:P ratios during the days of the experiment (DOE). Points are observations for each respective treatment (*Cntl* blue points; *HF* grey triangles; *L* yellow diamonds; *HFL* red squares). Green dashed horizontal line indicates the Redfield ratio (lnN:P = 2.77) and pink one the threshold elemental ratio for seston P nutrient deficiency, lnN:P > 3.09 (Healey & Hendzel, 1980). Black dashed vertical line indicates when the allo-OM pulse event occurred. Model summary output is in Table S3. *P*-values significant codes: < 0.001 = '***'; < 0.01 = '**'; < 0.05 = '*'; non-significant = ns

higher DOC pulse additions, the L treatment added more water colour than the HF treatment. Consequently, the L treatment behaved in a similar way to what was expected from the combined HFL treatment (i.e. an increase in water colour and DOC quantity). In turn, the HFL treatment experienced more than double the shading effects compared with the HF treatment. It is clear, therefore, that despite the initial intention of
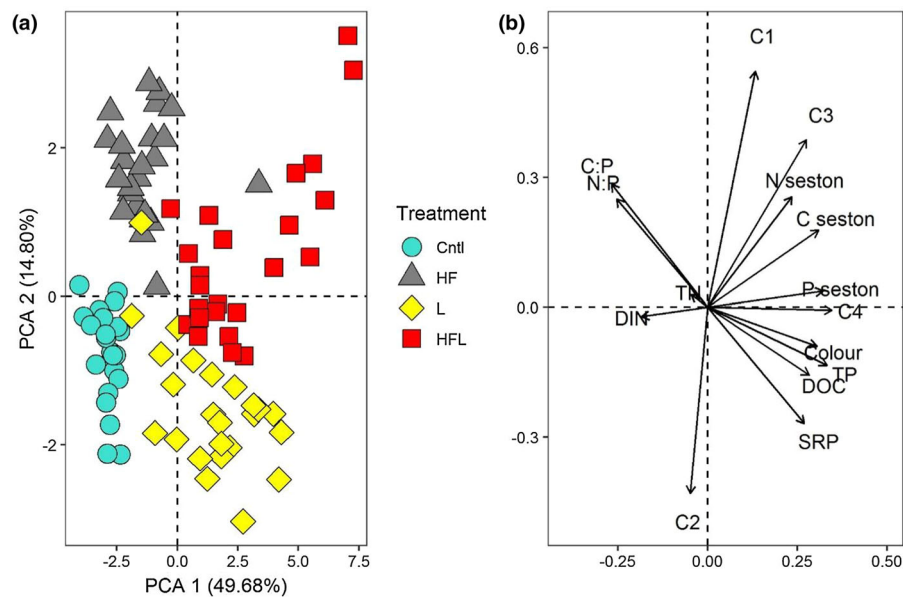
Fig. 6 PCA reveals differences in treatments (**a**) based on different carbon and nutrient quantity and quality water chemistry parameters (**b**). Symbols of different colours represent different treatment observations: *Cntl* blue points, *HF* grey triangles, *L* yellow diamonds, *HFL* red squares

the experimental design to increase DOC in the absence of significant increases in colour via the L treatment as per the methodology employed by Hitchcock et al. (2016), colour was, nevertheless, added in substantial concentrations. Colour is not always measured following additions of allo-OM leaf leachate sources in mesocosm experiments (Hitchcock et al., 2016). This may lead to erroneous conclusions regarding planktonic responses, as the effect of increased colour is not separated from effects of increased DOC in these cases. Colour associated with DOC additions from allo-OM sources such as leaf leachates should be determined prior to experimental additions to ensure that the effect of colour following allo-OM pulses can be appropriately assessed. In other studies, tested separate shading effects of leaf leachates as an added DOC source is not generally well achieved due to the use of covers as an extra treatment (Brighenti et al., 2018), which is different from adding colour to the water, or by using a completely different uncoloured labile DOC source such as sucrose as a comparable treatment (Geddes, 2015). On the other hand, there are also studies which only focus on the browning effects, without considering the quality and quantity of potential DOC added, such as when commercially available humic

substances are used (Rasconi et al., 2015; Urrutia-Cordero et al., 2017; Lebret et al., 2018). In our study, the aim to disentangle the independent and combined physical and chemical effects of browning (i.e. light limitation) and external energy exports (i.e. carbon and nutrient quantity) was also hardly achieved because of the unexpected high colour added with the leaf leachate source. Future studies investigating how different allo-OM sources impact aquatic ecosystems should more carefully consider DOC-colour relationships of these extracts and compare individual effects by adding the same amount of DOC or colour, aspect not considered in this work.

Seston elemental content and stoichiometry

Despite the large number of studies quantifying seston nutrient content and ratios in lakes (Prater et al., 2017; Bergström et al., 2018), direct analyses of this fraction in mesocosm studies are not that common (Schulhof et al., 2019; Minguez et al., 2020). In our study the HF treatment added seston N, also found in a recently published study (Minguez et al., 2020), whereas the alder tree leaf leachate source increased concentrations of P, as reported elsewhere (Mutschlecner et al., 2018; Navarro et al., 2019). As expected, the HF
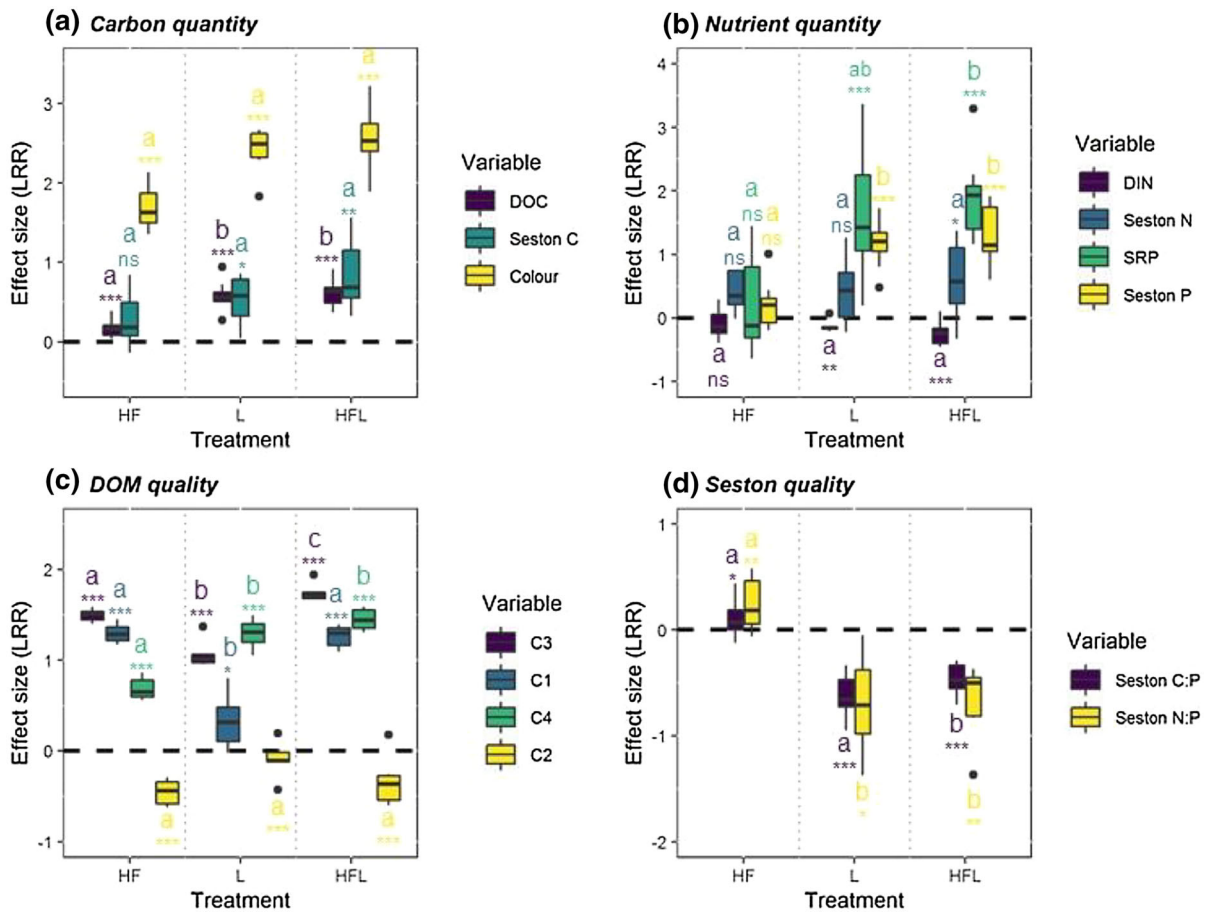
Fig. 7 Effect sizes (LRR) of the three different treatments to different water chemistry quantity and quality parameters. **a** Carbon quantity: DOC, seston C and colour; **b** nutrient quantity: DIN, seston N, SRP and seston P; **c** DOM quality: PARAFAC components; and **d** seston quality: C:P and N:P ratios. Dashed horizontal black lines at 0 indicate the general benchmark (notice than when available we used benchmark of day 0, close to 0 but not represented visually. See Table S4). *P*-values significant codes differing from benchmark values: $P < 0.001$ = '***'; $P < 0.01$ = '**'; $P < 0.05$ = '*'; $P > 0.05$ = 'ns', non-significant (Table S5). Different letters between treatments indicate significant differences (*P*-value < 0.05) amongst them (Table S6). Box = 25th and 75th percentiles, whiskers = 1.5*inter-quartile range. Black line = median

treatment enclosures had higher seston C:P ratios compared to the L and HFL treatments, similar to those found in other experiments using HuminFeed® as an allo-OM source analogue (Minguez et al., 2020). High seston C:P values were observed in the HF treatment, but also in the control treatments, implying potential nutrient constraints for primary consumers based on previously published seston nutrient ratio thresholds (Urabe & Watanabe, 1992). Moreover, high seston N:P values throughout the experimental period indicated that the HF and control mesocosms were under severe P limited conditions relative to N, even before starting the allo-OM additions and

contrasting with results reported by Minguez et al. (2020) who observed no P limitation in the HF treatment or in the unmanipulated control treatments. In our study, seston C:P and N:P ratios in treatments which received the leaf leachate source (L and HFL enclosures) were lower than the HF treatment. The nutrient concentrations and relative proportions of leaf leachates are highly variable and different from those found elsewhere in leaf litter from the same tree species (Osborne et al., 2007; Schreeg et al., 2013). Due to the higher solubility of P compared to N and C, it is common to observe greater influence of P in leaf
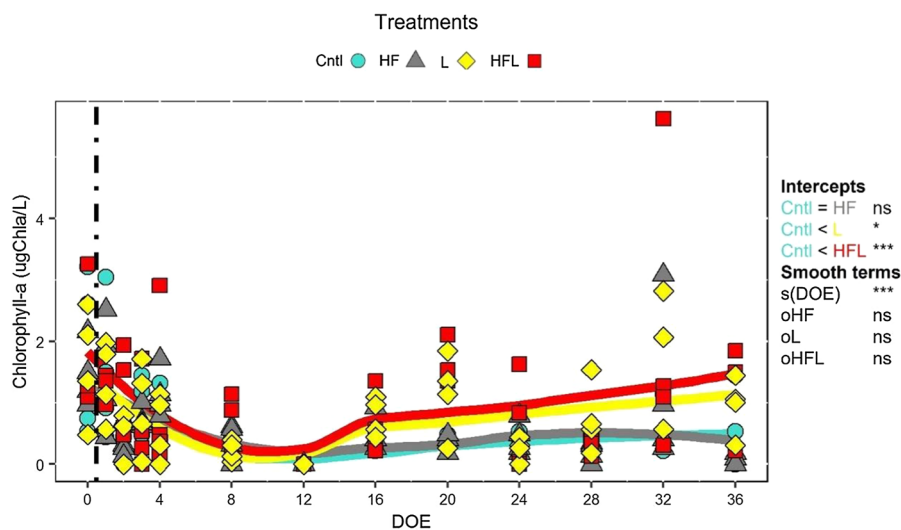
Fig. 8 GAM smoothers (solid lines) showing the temporal trends in Chl-*a* concentrations during the days of the experiment (DOE). Points are observations for each respective treatment (*Cntl* blue points; *HF* grey triangles; *L* yellow diamonds; *HFL* red squares). Black dashed vertical line indicates when the allo-OM pulse event occurred. Model summary output is in Table S7. *P*-values significant codes: < 0.001 = '***'; < 0.01 = '**'; < 0.05 = '*'; non-significant = ns

leachates directly affecting nutrient ratios (Schreeg et al., 2013).

Significant non-linear trends were observed for both ratios (C:P and N:P) during the 36 days of experiment. The pulse disturbance event clearly affected these nutrient ratio values. Seston C:P reached minimum values at day 4 but increased and stabilised again towards the end of the experiment. Similarly, seston N:P values were lowest directly following the allo-OM additions. In natural freshwater ecosystems, seston C:P and N:P ratios tend to decrease during mixing and the rainy season, or in autumn and winter, when there is likely a greater nutrient supply to the lake surface mixed layer as a consequence of increased fluvial inputs, whilst higher values are often associated with spring and summer (Prater et al., 2017; Ngochera & Bootsma, 2018). Most of these studies relate seasonal patterns in lake seston quality with changes in particulate P supply and subsequent P-uptake during the growing season, despite site-specific physical and biological drivers (Elser et al., 1995; Hessen et al., 2005). Overall, extensive temporal variations of these ratios suggest the need to better understand mechanistic changes in the biochemistry of lake seston (Kreeger et al., 1997; Calderó-Pascual et al., 2020). In our study, the unexpected decrease of seston C:P ratio in all treatments the first week after the pulse could be explained by 1) relatively high P

additions in the treatments receiving the P rich leaf leachate source and 2) the collapse of primary producers indicated by Chl-*a* in the control and HF mesocosms, which accounted for rapid declines in seston C relative to seston P. Seston C concentrations in the control enclosures gradually decreased during the experiment to below 0.5 mgC l^{-1}, the threshold at which *Daphnia* growth is considered food-limited (Lampert, 1987; Urabe et al., 2002). This suggests that regardless of food quality in terms of carbon constituents and elemental ratios, food quantity for primary consumers was likely to have declined in the control treatment as the experiment progressed to levels generally considered insufficient to support higher trophic levels. As the experiment progressed, increases in seston elemental ratios to pre-disturbance conditions, and even higher values, would suggest the uptake of the available dissolved P by primary consumers, which were likely already highly P limited even before the pulse disturbance event took place.

Mimic natural allo-OM sources

In our experiment, in an effort to mimic natural additions of nutrients following inputs of allo-OM and to optimise the number of treatments versus the number of replicates per treatment, inorganic nutrients were not added to match those introduced with the

HuminFeed® and leaf leachate sources, which contrasts with other authors who added inorganic nutrients to the enclosures (Lefébure et al., 2013; Geddes, 2015; Hitchcock et al., 2016; Urrutia-Cordero et al., 2017) or created an extra treatment controlling the single effect of nutrient additions (Brighenti et al., 2018). Consequently, in this study, the control and HF treatments experienced extreme P limitation over the course of the experiment, potentially masking the directly tested browning effects, as found in other studies (Tonetta et al., 2018). Prior to the described experiment, we aimed to prepare a local (i.e. top bare soil) allo-OM stock solution. However, it was logistically complex to obtain the designed high DOC concentrations for the targeted treatment. Therefore, for practical reasons, we collected alder tree leaves from a national park (40° 39′ 22.1" N, 31° 37′ 47.89" E), in Bolu, Turkey. This source is unlikely, therefore, to be directly representative of natural allo-OM additions to the lake in which the mesocosms were located. Efforts to mimic natural allo-OM additions would have been improved by preparing and characterising treatment stock solutions similar to the surroundings catchment sources. In turn, new studies considering other types of allo-OM such as agricultural soil (Liess et al., 2015), different types of leaf leachates (Lennon & Cottingham, 2008), and burned soil leachates (Cunillera-Montcusí et al., 2019) should be further explored as common catchment type systems affecting aquatic environments. However, more attention should be paid to mimicking natural inputs of DOM. Realistically, an increase of 8 mgC l^{-1} as DOC in pelagic systems is not a predicted scenario for lakes owing to higher buffering capacity and lower resident time (Leech et al., 2018) compared to concentration in streams, which often show high peaks in POC and DOC concentrations after flooding events (Dhillon & Inamdar, 2013; Hitchcock & Mitrovic, 2015). Other authors mimicking potential predicted scenarios ranged from + 1.2 to + 4.8 mgC l^{-1} (Sanders et al., 2015; Brighenti et al., 2018; Lebret et al., 2018), which places their maximum DOC additions at half the value of the additions with the leaf leachate source in this study which were used to follow intermediate concentrations used by Hitchcock et al, (2016).

Overall treatment effects

In this study, the LRR effect sizes approach recommended by Hillebrand & Gurevitch (2016) was utilised in order to contrast impacts of different allo-OM sources (i.e. examination of changes with reference to the control treatment). The HuminFeed® effects were mainly lower, and even non-statistically significant for some of the variables studied, compared to the stronger effects arising from the additions of the leaf leachate source. The only variables to have the same strong effects in the HF treatment as observed in the L treatment were DOM quality parameters (i.e. PARAFAC components). In turn, the HFL treatment experienced additive effects, which were different to our expectations of finding multiplicative influences on the outcomes. The HF treatment showed lower seston nutrient ratio effects relative to the L and HFL treatments. In addition, in this case, the HF treatment showed positive effects (i.e. increased overall seston C:P and N:P) whilst the L and HFL treatments' effects were negative (i.e. decreased overall seston C:P and N:P). For all these reasons, the overall effect sizes of the combined HFL treatment were mainly influenced by the presence of the leaf leachate source, since HuminFeed® acted more like the control and different from the expected synergistic effects of the combined sources.

Implications for primary productivity

Different from what we hypothesised, we found maximum Chl-*a* concentrations in the HFL treatment followed by the L treatment, whilst Chl-*a* concentrations and dynamics in the HF treatment did not differ from controls. Previous studies have simulated increases in water colour using HuminFeed® additions and have shown that, similar to what we found but different to what we expected, the respective percentage increase in water colour did not have any effect on total phytoplankton biomass (Ratcovich, 2014; Urrutia-Cordero et al., 2017; Lebret et al., 2018). Our results suggest that, as expected, primary producers were mainly stimulated by P additions associated with the leaf leachate source. Therefore, it would appear that the addition of nutrients exerted a greater influence than light reduction due to browning, as was also reported by other authors (Kankaala et al., 2010; Sanders et al., 2015; Hitchcock et al., 2016;

Degerman et al., 2018; Tonetta et al., 2018), and especially in already P limited ecosystems (Villar-Argaiz et al., 2018), as in our investigated system. In addition, although there was no phytoplankton community composition data available for our experiment, other authors found greater abundance of mixotrophic, e.g. Cryptophytes and nanoplanktonic flagellates in the enclosures receiving leaf leachate on top of HuminFeed® in contrast to clear controls and brown HF individual treatments (Fonseca et al., 2022). This would suggest that, in our study, a potential increase in mixotrophic algae in the treatments receiving the leaf leachate source could explain the unexpected maximum increase in Chl-*a* response in the HFL treatment. Regarding reported overall temporal dynamics, minimum Chl-*a* concentrations observed around day 12 in all mesocosms could be explained by high grazing pressure since the beginning of the experiment as this decrease does not seem to be related with differences in treatment water chemistry, but more influenced by biological interactions (Yıldız et al., in prep).

Conclusion

Alterations in the supply of allo-OM to freshwater lakes due to global change is evident. However, there is still considerable uncertainty in consolidating projected scenarios for in-lake processes. Our study highlights that it is important to characterise the resources used to mimic allo-OM inputs in mesocosm experiments in order to understand and predict the impacts to aquatic ecosystems. In this study, the fact that leaf leachate treatments added P to a likely P limited system suggests that allo-OM disturbance events could increase nutrient availability to nutrient limited planktonic communities, as observed in other temperate lakes (Senar et al., 2021). On the other hand, the same events could enhance eutrophication in water bodies which are already nutrient sufficient, as reported elsewhere (Gao et al., 2021). In contrast, other types of allo-OM sources, which are more similar to HuminFeed® characteristics, such as those associated with humic waters (Hamdan et al., 2021), could lead to higher nutrient constraints (i.e. high C relative to N and P) at all trophic levels. Our results demonstrated that, the HF treatment behaved as expected compared to the unexpected increases in water colour with the L treatment. In addition, the HF

treatment overall LRR effect sizes were weaker than expected, but stronger for the L treatment which added high amounts of P, adding complexity to the capacity of the experiment to disentangle browning effects from those of direct external C inputs effects. However, by characterising the nutrient components within the treatment, some of this complexity can be directly addressed. The indirect effect of nutrient stoichiometry associated with dissolved and particulate allo-OM inputs as well as DOM quality, in addition to browning and carbon quantity repercussions, are all key factors regulating the ecological responses to projected increases in allo-OM in freshwater systems and should be characterised in future mesocosm experiments.

Availability of data and material The datasets generated and analysed during the current study are available within this article and its supplementary information files through the presented figures and tables. Raw experimental metadata will be publicly available after three years of the experiment (i.e. 2023) through the AQUACOSM mesocosm data repository (https://www.aquacosm.eu/data/) but can be available from the corresponding authors on reasonable request.

Code availability All code available can be found in electronic supplementary material.

Declarations

Conflict of interest The authors declare no conflict of interest.

References

Alpert, P., T. Ben-Gai, A. Baharad, Y. Benjamini, D. Yekutieli, M. Colacino, L. Diodato, C. Ramis, V. Homar, R. Romero, S. Michaelides & A. Manes, 2002. The paradoxical increase of Mediterranean extreme daily rainfall in spite of decrease in total values. Geophysical Research Letters 29: 31-1-31–34.

Anderson, M. J., 2017. Permutational Multivariate Analysis of Variance (PERMANOVA) Wiley StatsRef: Statistics Reference Online. American Cancer Society: 1–15. https://doi.org/10.1002/9781118445112.stat07841.

Asam, Z.-U.-Z., 2012. Cycling and transport of phosphorus and nitrogen from harvested peatland forests and possible mitigation and methods. Civil Engineering Department, National University of Ireland, http://hdl.handle.net/10379/3431.

Baird, R. & L. Bridgewater, 2017. APHA. Standard Methods for the Examination of Water and Wastewater, American Public Health Association, Washington, DC:

Bergström, A.-K., J. Karlsson, D. Karlsson & T. Vrede, 2018. Contrasting plankton stoichiometry and nutrient regeneration in northern arctic and boreal lakes. Aquatic Sciences 80: 24.

Brett, M. T., M. J. Kainz, S. J. Taipale & H. Seshan, 2009. Phytoplankton, not allochthonous carbon, sustains herbivorous zooplankton production. Proceedings of the National Academy of Sciences National Academy of Sciences 106: 21197–21201.

Brighenti, L. S., P. A. Staehr, L. P. M. Brandão, F. A. R. Barbosa & J. F. Bezerra-Neto, 2018. Importance of nutrients, organic matter and light availability on epilimnetic metabolic rates in a mesotrophic tropical lake. Freshwater Biology 63: 1143–1160.

Buttigieg, P. L. & A. Ramette, 2014. A guide to statistical analysis in microbial ecology: a community-focused, living review of multivariate data analyses. FEMS Microbiology Ecology 90: 543–550.

Calderó-Pascual, M., E. de Eyto, E. Jennings, M. Dillane, M. R. Andersen, S. Kelly, H. L. Wilson & V. McCarthy, 2020. Effects of consecutive extreme weather events on a temperate Dystrophic Lake: a detailed insight into physical, chemical and biological responses. Water Multidisciplinary Digital Publishing Institute 12: 1411.

Caverly, E., J. M. Kaste, G. S. Hancock & R. M. Chambers, 2013. Dissolved and particulate organic carbon fluxes from an agricultural watershed during consecutive tropical storms. Geophysical Research Letters 40: 5147–5152.

Chai, L., M. Huang, H. Fan, J. Wang, D. Jiang, M. Zhang & Y. Huang, 2019. Urbanization altered regional soil organic matter quantity and quality: Insight from excitation emission matrix (EEM) and parallel factor analysis (PARAFAC). Chemosphere 220: 249–258.

Clarke, K. R., 1993. Non-parametric multivariate analyses of changes in community structure. Australian Journal of Ecology 18: 117–143.

Coble, P. G., 1996. Characterization of marine and terrestrial DOM in seawater using excitation-emission matrix spectroscopy. Marine Chemistry Elsevier 51: 325–346.

Cole, J. J., S. R. Carpenter, J. Kitchell, M. L. Pace, C. T. Solomon & B. Weidel, 2011. Strong evidence for terrestrial support of zooplankton in small lakes based on stable isotopes of carbon, nitrogen, and hydrogen. Proceedings of the National Academy of Sciences National Academy of Sciences 108: 1975–1980.

Cooke, S. L., J. M. Fischer, K. Kessler, C. E. Williamson, R. W. Sanders, D. P. Morris, J. A. Porter, W. H. Jeffrey, S. D. Princiotta & J. D. Pakulski, 2015. Direct and indirect effects of additions of chromophoric dissolved organic matter on zooplankton during large-scale mesocosm experiments in an oligotrophic lake. Freshwater Biology 60: 2362–2378.

Cory, R. M., B. C. Crump, J. A. Dobkowski & G. W. Kling, 2013. Surface exposure to sunlight stimulates CO2 release from permafrost soil carbon in the Arctic. Proceedings of the National Academy of Sciences National Academy of Sciences 110: 3429–3434.

Cramer, W., J. Guiot, M. Fader, J. Garrabou, J.-P. Gattuso, A. Iglesias, M. A. Lange, P. Lionello, M. C. Llasat, S. Paz, J. Peñuelas, M. Snoussi, A. Toreti, M. N. Tsimplis & E. Xoplaki, 2018. Climate change and interconnected risks to sustainable development in the Mediterranean. Nature Climate Change 8: 972–980.

Creed, I. F., A.-K. Bergström, C. G. Trick, N. B. Grimm, D. O. Hessen, J. Karlsson, K. A. Kidd, E. Kritzberg, D. M. McKnight, E. C. Freeman, O. E. Senar, A. Andersson, J. Ask, M. Berggren, M. Cherif, R. Giesler, E. R. Hotchkiss,

P. Kortelainen, M. M. Palta, T. Vrede & G. A. Weyhenmeyer, 2018. Global change-driven effects on dissolved organic matter composition: Implications for food webs of northern lakes. Global Change Biology 24: 3692–3714.

Cunillera-Montcusí, D., S. Gascón, I. Tornero, J. Sala, N. Àvila, X. D. Quintana & D. Boix, 2019. Direct and indirect impacts of wildfire on faunal communities of Mediterranean temporary ponds. Freshwater Biology 64: 323–334.

Cuss, C. W., & C. Guéguen, 2015. Characterizing the Labile Fraction of Dissolved Organic Matter in Leaf Leachates: Methods, Indicators, Structure, and Complexity Labile Organic Matter—Chemical Compositions, Function, and Significance in Soil and the Environment. Wiley: 237–274. https://doi.org/10.2136/sssaspecpub62.2014.0043.

de Wit, H. A., S. Valinia, G. A. Weyhenmeyer, M. N. Futter, P. Kortelainen, K. Austnes, D. O. Hessen, A. Räike, H. Laudon & J. Vuorenmaa, 2016. Current browning of surface waters will be further promoted by wetter climate. Environmental Science & Technology Letters American Chemical Society 3: 430–435.

Degerman, R., R. Lefébure, P. Byström, U. Båmstedt, S. Larsson & A. Andersson, 2018. Food web interactions determine energy transfer efficiency and top consumer responses to inputs of dissolved organic carbon. Hydrobiologia 805: 131–146.

Derrien, M., M.-S. Kim, G. Ock, S. Hong, J. Cho, K.-H. Shin & J. Hur, 2018. Estimation of different source contributions to sediment organic matter in an agricultural-forested watershed using end member mixing analyses based on stable isotope ratios and fluorescence spectroscopy. Science of the Total Environment 618: 569–578.

Dhillon, G. S. & S. Inamdar, 2013. Extreme storms and changes in particulate and dissolved organic carbon in runoff: entering uncharted waters? Geophysical Research Letters 40: 1322–1327.

von Einem, J. & W. Granéli, 2010. Effects of fetch and dissolved organic carbon on epilimnion depth and light climate in small forest lakes in southern Sweden. Limnology and Oceanography 55: 920–930.

Elser, J. J., T. H. Chrzanowski, R. W. Sterner, J. H. Schampel & D. K. Foster, 1995. Elemental ratios and the uptake and release of nutrients by phytoplankton and bacteria in three lakes of the Canadian shield. Microbial Ecology 29: 145–162.

Fellman, J. B., E. Hood & R. G. M. Spencer, 2010. Fluorescence spectroscopy opens new windows into dissolved organic matter dynamics in freshwater ecosystems: a review. Limnology and Oceanography 55: 2452–2462.

Findlay, S. & R. L. Sinsabaugh, 2003. Aquatic Ecosystems: Interactivity of Dissolved Organic Matter, Academic Press, Amsterdam:

Fonseca, B. M., E. E. Levi, L. W. Jensen, D. Graeber, M. Søndergaard, T. L. Lauridsen, E. Jeppesen & T. A. Davidson, 2022. Effects of DOC addition from different sources on phytoplankton community in a temperate eutrophic lake: an experimental study exploring lake compartments. Science of The Total Environment 803: 150049.

Gao, X., H. Chen, B. Gu, E. Jeppesen, Y. Xue & J. Yang, 2021. Particulate organic matter as causative factor to eutrophication of subtropical deep freshwater: role of typhoon (tropical cyclone) in the nutrient cycling. Water Research 188: 116470.

Ged, E. C. & T. H. Boyer, 2013. Molecular weight distribution of phosphorus fraction of aquatic dissolved organic matter. Chemosphere 91: 921–927.

Geddes, P., 2015. Experimental evidence that subsidy quality affects the temporal variability of recipient zooplankton communities. Aquatic Sciences 77: 609–621.

Guillemette, F., S. L. McCallister & P. A. del Giorgio, 2016. Selective consumption and metabolic allocation of terrestrial and algal carbon determine allochthony in lake bacteria. The ISME Journal Nature 10: 1373–1382.

Hamdan, M., P. Byström, E. R. Hotchkiss, M. J. Al-Haidarey & J. Karlsson, 2021. An experimental test of climate change effects in northern lakes: Increasing allochthonous organic matter and warming alters autumn primary production. Freshwater Biology. https://doi.org/10.1111/fwb.13679.

Harris, D., W. R. Horwáth & C. van Kessel, 2001. Acid fumigation of soils to remove carbonates prior to total organic carbon or CARBON-13 isotopic analysis. Soil Science Society of America Journal 65: 1853–1856.

Healey, F. P. & L. L. Hendzel, 1980. Physiological indicators of nutrient deficiency in Lake Phytoplankton. Canadian Journal of Fisheries and Aquatic Sciences 37: 442–453.

Heckler, C. E., 2005. Applied multivariate statistical analysis. Technometrics 47: 517–517.

Hecky, R. E., P. Campbell & L. L. Hendzel, 1993. The stoichiometry of carbon, nitrogen, and phosphorus in particulate matter of lakes and oceans. Limnology and Oceanography 38: 709–724.

Hessen, D. O., E. van Donk & R. Gulati, 2005. Seasonal seston stoichiometry: effects on zooplankton in cyanobacteria-dominated lakes. Journal of Plankton Research 27: 449–460.

Hillebrand, H. & J. Gurevitch, 2016. Meta-Analysis and Systematic Reviews in Ecology eLS: 1–11.

Hillebrand, H., S. Langenheder, K. Lebret, E. Lindström, Ö. Östman & M. Striebel, 2018. Decomposing multiple dimensions of stability in global change experiments. Ecology Letters 21: 21–30.

Hitchcock, J. N. & S. M. Mitrovic, 2015. Highs and lows: the effect of differently sized freshwater inflows on estuarine carbon, nitrogen, phosphorus, bacteria and chlorophyll a dynamics. Estuarine, Coastal and Shelf Science 156: 71–82.

Hitchcock, J. N., S. M. Mitrovic, W. L. Hadwen, D. L. Roelke, I. O. Growns & A.-M. Rohlfs, 2016. Terrestrial dissolved organic carbon subsidizes estuarine zooplankton: an in situ mesocosm study. Limnology and Oceanography 61: 254–267.

Hope, D., M. F. Billett & M. S. Cresser, 1994. A review of the export of carbon in river water: fluxes and processes. Environmental Pollution 84: 301–324.

Isles, P. D. F., 2020. The misuse of ratios in ecological stoichiometry. Ecology 101: e03153.

Jaffé, R., K. M. Cawley & Y. Yamashita, 2014. Applications of excitation emission matrix fluorescence with parallel factor analysis (EEM-PARAFAC) in assessing environmental dynamics of natural dissolved organic matter (DOM) in aquatic environments: a review advances in the physico-chemical characterization of dissolved organic matter:

impact on natural and engineered systems. American Chemical Society. https://doi.org/10.1021/bk-2014-1160.ch003.

Jeong, J.-J., S. Bartsch, J. H. Fleckenstein, E. Matzner, J. D. Tenhunen, S. D. Lee, S. K. Park & J.-H. Park, 2012. Differential storm responses of dissolved and particulate organic carbon in a mountainous headwater stream, investigated by high-frequency, in situ optical measurements. Journal of Geophysical Research: Biogeosciences. https://doi.org/10.1029/2012JG001999.

Jespersen, A.-M. & K. Christoffersen, 1987. Measurements of chlorophyll-a from phytoplankton using ethanol as extraction solvent. Archiv Für Hydrobiologie 109: 445–454.

Kankaala, P., S. Peura, H. Nykänen, E. Sonninen, S. Taipale, M. Tiirola & R. I. Jones, 2010. Impacts of added dissolved organic carbon on boreal freshwater pelagic metabolism and food webs in mesocosm experiments. Fundamental and Applied Limnology/Archiv Für Hydrobiologie 177: 161–176.

Kassambara, A., 2020. Pipe-Friendly Framework for Basic Statistical Tests, R Foundation for Statistical Computing, Vienna:

Kellerman, A. M., T. Dittmar, D. N. Kothawala & L. J. Tranvik, 2014. Chemodiversity of dissolved organic matter in lakes driven by climate and hydrology. Nature Communications Nature Publishing Group 5: 3804.

Kelly, P. T., W. H. Renwick, L. Knoll & M. J. Vanni, 2019. Stream nitrogen and phosphorus loads are differentially affected by storm events and the difference may be exacerbated by conservation tillage. Environmental Science & Technology American Chemical Society 53: 5613–5621.

Kida, M., T. Kojima, Y. Tanabe, K. Hayashi, S. Kudoh, N. Maie & N. Fujitake, 2019. Origin, distributions, and environmental significance of ubiquitous humic-like fluorophores in Antarctic lakes and streams. Water Research 163: 114901.

Kothawala, D. N., C. A. Stedmon, R. A. Müller, G. A. Weyhenmeyer, S. J. Köhler & L. J. Tranvik, 2014. Controls of dissolved organic matter quality: evidence from a large-scale boreal lake survey. Global Change Biology 20: 1101–1114.

Kreeger, D., C. Goulden, S. Kilham, S. Lynn, S. Datta & S. Interlandi, 1997. Seasonal changes in the biochemistry of lake seston. Freshwater Biology 38: 539–554.

Lampert, W., 1987. Feeding and nutrition in Daphnia. Daphnia 143–192.

Landkildehus, F., M. Søndergaard, M. Beklioglu, R. Adrian, D. G. Angeler, J. Hejzlar, E. Papastergiadou, P. Zingel, A. IdilÇakiroğlu, U. Scharfenberger, S. Drakare, T. Nõges, M. Sorf, K. Stefanidis, Ü. N. Tavşanoğlu, C. Trigal, A. Mahdy, C. Papadaki, L. Tuvikene, S. E. Larsen, M. Kernan & E. Jeppesen, 2014. Climate change effects on shallow lakes: design and preliminary results of a cross-European climate gradient mesocosm experiment. Estonian Journal of Ecology 63: 71.

Lebret, K., S. Langenheder, N. Colinas, Ö. Östman & E. S. Lindström, 2018. Increased water colour affects freshwater plankton communities in a mesocosm study. Aquatic Microbial Ecology 81: 1–17.

Leech, D. M., A. I. Pollard, S. G. Labou & S. E. Hampton, 2018. Fewer blue lakes and more murky lakes across the continental US: implications for planktonic food webs. Limnology and Oceanography 63: 2661–2680.

Lefébure, R., R. Degerman, A. Andersson, S. Larsson, L.-O. Eriksson, U. Båmstedt & P. Byström, 2013. Impacts of elevated terrestrial nutrient loads and temperature on pelagic food-web efficiency and fish production. Global Change Biology 19: 1358–1372.

Lennon, J. T. & K. L. Cottingham, 2008. Microbial productivity in variable resource environments. Ecology 89: 1001–1014.

Lennon, J. T., S. K. Hamilton, M. E. Muscarella, A. S. Grandy, K. Wickings & S. E. Jones, 2013. A source of terrestrial organic carbon to investigate the browning of aquatic ecosystems. PLoS ONE 8: e75771.

Liess, A., C. Faithfull, B. Reichstein, O. Rowe, J. Guo, R. Pete, G. Thomsson, W. Uszko & S. N. Francoeur, 2015. Terrestrial runoff may reduce microbenthic net community productivity by increasing turbidity: a Mediterranean coastal lagoon mesocosm experiment. Hydrobiologia 753: 205–218.

Mackerth, F., 1978. Water analysis: some revised methods for limnologists. Freshwater Biological Association 36: 117.

Martinez Arbizu, P., 2017. pairwiseAdonis: Pairwise multilevel comparison using adonis. R package version 0.0 1.

McCarthy, V., I. A. N. Donohue & K. Irvine, 2006. Field evidence for stoichiometric relationships between zooplankton and N and P availability in a shallow calcareous lake. Freshwater Biology 51: 1589–1604.

McKnight, D. M., E. W. Boyer, P. K. Westerhoff, P. T. Doran, T. Kulbe & D. T. Andersen, 2001. Spectrofluorometric characterization of dissolved organic matter for indication of precursor organic material and aromaticity. Limnology and Oceanography 46: 38–48.

Mcmeans, B. C., A.-M. Koussoroplis, M. T. Arts & M. J. Kainz, 2015. Terrestrial dissolved organic matter supports growth and reproduction of Daphnia magna when algae are limiting. Journal of Plankton Research Oxford Academic 37: 1201–1209.

Meinelt, T., A. Paul, T. M. Phan, E. Zwirnmann, A. Krüger, A. Wienke & C. E. W. Steinberg, 2007. Reduction in vegetative growth of the water mold Saprolegnia parasitica (Coker) by humic substance of different qualities. Aquatic Toxicology 83: 93–103.

Minguez, L., E. Sperfeld, S. A. Berger, J. C. Nejstgaard & M. O. Gessner, 2020. Changes in food characteristics reveal indirect effects of lake browning on zooplankton performance. Limnology and Oceanography 65: 1028–1040.

Monteith, D. T., J. L. Stoddard, C. D. Evans, H. A. de Wit, M. Forsius, T. Høgåsen, A. Wilander, B. L. Skjelkvåle, D. S. Jeffries, J. Vuorenmaa, B. Keller, J. Kopácek & J. Vesely, 2007. Dissolved organic carbon trends resulting from changes in atmospheric deposition chemistry. Nature Nature Publishing Group 450: 537–540.

Murphy, K. R., C. A. Stedmon, D. Graeber & R. Bro, 2013. Fluorescence spectroscopy and multi-way techniques. PARAFAC. Analytical Methods Royal Society of Chemistry 5: 6557–6566.

Mutschlecner, A. E., J. J. Guerard, J. B. Jones & T. K. Harms, 2018. Phosphorus enhances uptake of dissolved organic matter in Boreal streams. Ecosystems 21: 675–688.

Navarro, M. B., V. D. Villanueva & B. Modenutti, 2019. High phosphorus content in leachates of the austral beech Nothofagus pumilio stimulates bacterioplankton C-consumption. Freshwater Science the University of Chicago Press 38: 435–447.

Ngochera, M. J. & H. A. Bootsma, 2018. Carbon, nitrogen and phosphorus content of seston and zooplankton in tropical Lake Malawi: implications for zooplankton nutrient cycling. Aquatic Ecosystem Health & Management Taylor & Francis 21: 185–192.

Nicolle, A., P. Hallgren, J. V. Einem, E. S. Kritzberg, W. Granéli, A. Persson, C. Brönmark & L.-A. Hansson, 2012. Predicted warming and browning affect timing and magnitude of plankton phenological events in lakes: a mesocosm study. Freshwater Biology 57: 684–695.

Oksanen, J., 2011. Multivariate analysis of ecological communities in R: vegan tutorial. R Package Version 1: 1–43.

Osborne, T. Z., P. W. Inglett & K. R. Reddy, 2007. The use of senescent plant biomass to investigate relationships between potential particulate and dissolved organic matter in a wetland ecosystem. Aquatic Botany 86: 53–61.

Osburn, C. L., N. J. Anderson, C. A. Stedmon, M. E. Giles, E. J. Whiteford, T. J. McGenity, A. J. Dumbrell & G. J. C. Underwood, 2017. Shifts in the source and composition of dissolved organic matter in Southwest Greenland Lakes along a regional hydro-climatic gradient. Journal of Geophysical Research: Biogeosciences 122: 3431–3445.

Pedersen, E. J., D. L. Miller, G. L. Simpson, & N. Ross, 2019. Hierarchical generalized additive models in ecology: an introduction with mgcv. PeerJ PeerJ Inc. 7: e6876.

Prater, C., P. C. Frost, E. T. Howell, S. B. Watson, A. Zastepa, S. S. E. King, R. J. Vogt & M. A. Xenopoulos, 2017. Variation in particulate C: N: P stoichiometry across the Lake Erie watershed from tributaries to its outflow. Limnology and Oceanography 62: S194–S206.

Qualls, R. G. & C. J. Richardson, 2003. Factors controlling concentration, export, and decomposition of dissolved organic nutrients in the Everglades of Florida. Biogeochemistry 62: 197–229.

Quante, M. & F. Colijn, 2016. North Sea Region Climate Change Assessment, SpringerOpen, Cham:

R Core Team., 2019. R: A Language and Environment for Statistical Computing, R Foundation for Statistical Computing, Vienna:

Rasconi, S., A. Gall, K. Winter & M. J. Kainz, 2015. Increasing water temperature triggers dominance of small freshwater plankton. PLoS ONE 10: e0140449.

Ratcovich, J., 2014. The impact of climate change and brownification on primary and bacterial production. http://lup.lub.lu.se/student-papers/record/4333096.

Rose, N. L., H. Yang, S. D. Turner & G. L. Simpson, 2012. An assessment of the mechanisms for the transfer of lead and mercury from atmospherically contaminated organic soils to lake sediments with particular reference to Scotland, UK. Geochimica Et Cosmochimica Acta 82: 113–135.

Sanders, R. W., S. L. Cooke, J. M. Fischer, S. B. Fey, A. W. Heinze, W. H. Jeffrey, A. L. Macaluso, R. E. Moeller, D. P. Morris, P. J. Neale, M. H. Olson, J. D. Pakulski, J.

A. Porter, D. M. Schoener & C. E. Williamson, 2015. Shifts in microbial food web structure and productivity after additions of naturally occurring dissolved organic matter: Results from large-scale lacustrine mesocosms. Limnology and Oceanography 60: 2130–2144.

Schreeg, L. A., M. C. Mack & B. L. Turner, 2013. Nutrient-specific solubility patterns of leaf litter across 41 lowland tropical woody species. Ecology 94: 94–105.

Schulhof, M. A., J. B. Shurin, S. A. J. Declerck & D. B. V. de Waal, 2019. Phytoplankton growth and stoichiometric responses to warming, nutrient addition and grazing depend on lake productivity and cell size. Global Change Biology 25: 2751–2762.

Sebestyen, S. D., E. W. Boyer, J. B. Shanley, C. Kendall, D. H. Doctor, G. R. Aiken & N. Ohte, 2008. Sources, transformations, and hydrological processes that control stream nitrate and dissolved organic matter concentrations during snowmelt in an upland forest. Water Resources Research. https://doi.org/10.1029/2008WR006983.

Senar, O. E., I. F. Creed & C. G. Trick, 2021. Lake browning may fuel phytoplankton biomass and trigger shifts in phytoplankton communities in temperate lakes. Aquatic Sciences 83: 21.

Solomon, C. T., S. E. Jones, B. C. Weidel, I. Buffam, M. L. Fork, J. Karlsson, S. Larsen, J. T. Lennon, J. S. Read, S. Sadro & J. E. Saros, 2015. Ecosystem consequences of changing inputs of terrestrial dissolved organic matter to lakes: current knowledge and future challenges. Ecosystems 18: 376–389.

Stadler, M., E. Ejarque & M. J. Kainz, 2020. In-lake transformations of dissolved organic matter composition in a subalpine lake do not change its biodegradability. Limnology and Oceanography 65: 1554–1572.

Stedmon, C. A. & S. Markager, 2005. Resolving the variability in dissolved organic matter fluorescence in a temperate estuary and its catchment using PARAFAC analysis. Limnology and Oceanography 50: 686–697.

Sterner, R. W. & J. J. Elser, 2002. Ecological Stoichiometry: The Biology of Elements from Molecules to the Biosphere, Princeton University Press, Princeton:

Tanentzap, A. J., B. W. Kielstra, G. M. Wilkinson, M. Berggren, N. Craig, P. A. del Giorgio, J. Grey, J. M. Gunn, S. E. Jones, J. Karlsson, C. T. Solomon & M. L. Pace, 2017. Terrestrial support of lake food webs: Synthesis reveals controls over cross-ecosystem resource use. Science Advances American Association for the Advancement of Science 3: e1601765.

The Math Works, Inc., 2020. MATLAB.

Thurman, E. M., 1985. Aquatic humic substances. In Thurman, E. M. (ed), Organic Geochemistry of Natural Waters Springer, Dordrecht: 273–361.

Tonetta, D., P. A. Staehr, B. Obrador, L. P. M. Brandão, L. S. Brighenti, M. M. Petrucio, F. A. R. Barbosa & J. F. Bezerra-Neto, 2018. Effects of nutrients and organic matter inputs in the gases CO2 and O2: A mesocosm study in a tropical lake. Limnologica 69: 1–9.

Toreti, A., P. Naveau, M. Zampieri, A. Schindler, E. Scoccimarro, E. Xoplaki, H. A. Dijkstra, S. Gualdi & J. Luterbacher, 2013. Projections of global changes in precipitation extremes from Coupled Model Intercomparison Project

Phase 5 models. Geophysical Research Letters 40: 4887–4892.

Trenberth, K. E., 2011. Changes in precipitation with climate change. Climate Research 47: 123–138.

Urabe, J., M. Kyle, W. Makino, T. Yoshida, T. Andersen & J. J. Elser, 2002. Reduced light increases herbivore production due to stoichiometric effects of light/nutrient balance. Ecology 83: 619–627.

Urabe, J. & Y. Watanabe, 1992. Possibility of N or P limitation for planktonic cladocerans: an experimental test. Limnology and Oceanography 37: 244–251.

Urrutia-Cordero, P., M. K. Ekvall, J. Ratcovich, M. Soares, S. Wilken, H. Zhang & L.-A. Hansson, 2017. Phytoplankton diversity loss along a gradient of future warming and brownification in freshwater mesocosms. Freshwater Biology 62: 1869–1878.

Vad, C. F., C. Schneider, D. Lukić, Z. Horváth, M. J. Kainz, H. Stibor & R. Ptacnik, 2020. Grazing resistance and poor food quality of a widespread mixotroph impair zooplankton secondary production. Oecologia 193: 489–502.

Villar-Argaiz, M., E. G. Balseiro, B. E. Modenutti, M. S. Souza, F. J. Bullejos, J. M. Medina-Sánchez & P. Carrillo, 2018. Resource versus consumer regulation of phytoplankton: testing the role of UVR in a Southern and Northern hemisphere lake. Hydrobiologia 816: 107–120.

Weyhenmeyer, G. A., R. A. Müller, M. Norman & L. J. Tranvik, 2016. Sensitivity of freshwaters to browning in response to future climate change. Climatic Change 134: 225–239.

Wheeler, K. I., D. F. Levia & J. E. Hudson, 2017. Tracking senescence-induced patterns in leaf litter leachate using parallel factor analysis (PARAFAC) modeling and self-organizing maps. Journal of Geophysical Research: Biogeosciences 122: 2233–2250.

Wood, S. N., 2017. Generalized Additive Models: An Introduction with R, 2nd ed. CRC Press, Boca Raton:

Wood, S. & M. S. Wood, 2015. Package 'mgcv.' R Package Version 1: 29.

Wyatt, K. H. & A. R. Rober, 2020. Warming enhances the stimulatory effect of algal exudates on dissolved organic carbon decomposition. Freshwater Biology 65: 1288–1297.

Zhou, L., Y. Zhou, X. Tang, Y. Zhang, K.-S. Jang, A. J. Székely & E. Jeppesen, 2021. Resource aromaticity affects bacterial community successions in response to different sources of dissolved organic matter. Water Research 190: 116776.

Zhou, Y., M. Liu, L. Zhou, K.-S. Jang, H. Xu, K. Shi, G. Zhu, M. Liu, J. Deng, Y. Zhang, R. G. M. Spencer, D. N. Kothawala, E. Jeppesen & F. Wu, 2020. Rainstorm events shift the molecular composition and export of dissolved organic matter in a large drinking water reservoir in China: High frequency buoys and field observations. Water Research 187: 116471.

Zhou, Y., X. Yao, L. Zhou, Z. Zhao, X. Wang, K.-S. Jang, W. Tian, Y. Zhang, D. C. Podgorski, R. G. M. Spencer, D. N. Kothawala, E. Jeppesen, & F. Wu, 2021b. How hydrology and anthropogenic activity influence the molecular composition and export of dissolved organic matter: Observations along a large river continuum. Limnology and Oceanography n/a:, https://aslopubs.onlinelibrary.wiley.com/doi/abs/https://doi.org/10.1002/lno.11716.

Zuur, A., E. N. Ieno, N. Walker, A. A. Saveliev, & G. M. Smith, 2009. Mixed Effects Models and Extensions in Ecology with R. Springer Science & Business Media.